

Forensic identification of twin siblings and sex by digital palatal morphology

Ph.D. Thesis

Botond Barna Simon

Károly Rácz Doctoral School of Clinical Medicine
Semmelweis University



Supervisor: János Vág, D.M.D, Ph.D, Habil.

Official Reviewers: Bence Tamás Szabó, D.M.D, Ph.D

Márk Tibor Fráter, D.M.D, Ph.D, Habil, MSc.

Head of the Complex Examination Committee:

István Gera, D.M.D, Ph.D.

Members of the Complex Examination Committee:

Árpád Joób-Fancsali, D.M.D, Ph.D.

Zoltán Rakonczay, M.D., Ph.D.

Budapest

2023

TABLE OF CONTENTS

LIST OF ABBREVIATIONS	4
PREAMBLE	5
1. INTRODUCTION	7
1.1 MORPHOLOGY OF THE PALATE AND RUGAE TO ESTABLISH IDENTITY	7
1.1.1 <i>Distinguishing the sex in forensic odontology</i>	8
1.2 INTRAORAL SCANNERS	8
1.3 FORENSIC IDENTIFICATION.....	9
1.3.1 <i>The challenges of victim identification</i>	9
1.3.2 <i>Obstacles in the use of biometric identifiers</i>	11
1.3.3 <i>Dental records in forensic</i>	12
1.3.4 <i>Identification of twins and their role in forensic sciences</i>	12
2. OBJECTIVES	14
2.1 APPLICATION OF IOS TO IDENTIFY MONOZYGOTIC TWINS	14
2.2 THE DISCRIMINATIVE POTENTIAL OF PALATAL GEOMETRIC ANALYSIS FOR SEX DISCRIMINATION AND HUMAN IDENTIFICATION.....	14
3. METHODS	15
3.1 RECRUITED TWIN POPULATION.....	15
3.1.1 <i>Determination of zygosity</i>	15
3.2 APPLICATION OF IOS TO IDENTIFY MONOZYGOTIC TWINS	15
3.2.1 <i>Study subjects</i>	15
3.2.2 <i>Data acquisition</i>	16
3.2.3 <i>Alignment methods and surface comparison</i>	16
3.2.3 <i>Statistical analysis</i>	17
3.3 THE DISCRIMINATIVE POTENTIAL OF PALATAL GEOMETRIC ANALYSIS FOR SEX DISCRIMINATION AND HUMAN IDENTIFICATION.....	18
3.3.1 <i>Study subjects</i>	18
3.3.2 <i>The effect of the surface morphology (rugae) on MAD, smoothing the palate</i>	18
3.3.3 <i>Geometric measurement of the palate</i>	19
3.3.4 <i>Statistical analysis</i>	20
4. RESULTS	22
4.1 APPLICATION OF IOS TO IDENTIFY MONOZYGOTIC TWINS	22

4.1.1	<i>Repeatability (precision) of palatal intraoral scan</i>	22
4.1.2	<i>The deviation of palatal scans between MZ siblings</i>	22
4.1.3	<i>The probability of distinguishing between MZ siblings</i>	23
4.1.4	<i>The probability of distinguishing between MZ and DZ twins</i>	24
4.1.5	<i>Effect of age on ITD</i>	25
4.2	THE DISCRIMINATIVE POTENTIAL OF PALATAL GEOMETRIC ANALYSIS FOR SEX DISCRIMINATION AND HUMAN IDENTIFICATION	27
4.2.1	<i>The contribution of the surface morphology to the discriminative potential of the palate</i>	27
4.2.2	<i>Reliability of palatal geometry measurement</i>	28
4.2.3	<i>Comparison of the geometry between sexes</i>	28
4.2.4	<i>Correlation between geometry parameters</i>	29
4.2.5	<i>Linear discriminant analysis for sex prediction</i>	29
4.2.6	<i>The discriminant function of geometry parameters for identification</i>	30
5.	DISCUSSION	32
5.1	APPLICATION OF INTRAORAL SCANNER TO IDENTIFY MONOZYGOTIC TWINS	32
5.2	THE DISCRIMINATIVE POTENTIAL OF PALATAL GEOMETRIC ANALYSIS FOR SEX DISCRIMINATION AND HUMAN IDENTIFICATION	35
5.2.1	<i>Ethnicity and Palatal Metrics</i>	36
5.2.2	<i>Use of Geometric Measurement for Human Identification</i>	37
5.2.3	<i>Our advances in Palatoprint concept</i>	37
6.	CONCLUSIONS	40
6.1	APPLICATION OF INTRAORAL SCANNER TO IDENTIFY MONOZYGOTIC TWINS	40
6.2	THE DISCRIMINATIVE POTENTIAL OF PALATAL GEOMETRIC ANALYSIS FOR SEX DISCRIMINATION AND HUMAN IDENTIFICATION	40
7.	SUMMARY	41
8.	REFERENCES	42
9.	BIBLIOGRAPHY OF THE CANDIDATE'S PUBLICATIONS	52
PUBLICATIONS DIRECTLY CONNECTED TO THE DISSERTATION		52
<i>In 2022</i>		52
<i>In 2020</i>		52
PUBLICATIONS INDIRECTLY CONNECTED TO THE DISSERTATION		52
<i>In 2023</i>		52
<i>In 2022</i>		53
<i>In 2021</i>		53

<i>In 2020</i>	53
<i>In 2019</i>	54
<i>In 2018</i>	54
10. ACKNOWLEDGEMENTS	55

List of Abbreviations

DNA - Deoxyribonucleic acid
DVI – Disaster Victim Identification
DZ – Dizygotic
DZOS – Opposite-sex Dizygotic
DZSS – Same-sex Dizygotic
ICC – Intraclass correlation coefficient
IOS – Intraoral scanner
ISD – Intra-Subject Deviation
ITD – Inter-Twin Deviation
LM – Left Molar
LDA – Linear discriminant analysis
MAD – Mean Absolute Distance
MZ – Monozygotic
RM – Right Molar
SD – Standard Deviation
SE – Standard error of the mean
SEM – Standard error of measurement
STL – Standard triangulation language
TEM – Technical error of measurement
% TEM – Relative TEM

Preamble

Disaster Victim Identification (DVI) is a complex process that encompasses the identification of victims in various contexts, including mass disasters such as natural disasters, plane crashes, and terrorist attacks, as well as other cases involving convicted individuals, such as sexual abuse or murder. Mass disaster can be interpreted when as an event resulting in numerous victims ranging from tens to hundreds of thousands, depending on the nature of the disaster. Three main determinative aspects of human identification— deoxyribonucleic acid (DNA), odontology, and fingerprints—play a crucial role in distinguishing between individuals, especially in cases where traditional identification methods are inconclusive or unavailable. However, the identification of twins through DNA profiling can be challenging due to shared genetic markers, making it necessary for forensic experts to rely on additional factors like dental records, medical records, or personal effects to accurately differentiate between them and successfully identify the victims and giving closure for their families.

The continuous influx of illegal migrants attempting to enter Hungary has placed considerable pressure on the police, particularly since 2015 and further intensified by the Russian-Ukrainian war that began in February 2022. While efforts have been made to prevent illegal border crossings, the challenge lies in the lack of identification documents among migrants, making accurate identification and age assessment difficult. This issue has been exacerbated by false statements made by migrants. Migration concerns in the European Union since 2015 have also been linked to terrorist attacks. Forensic science extends beyond mass disasters and plays a significant role in identifying serial killers, perpetrators of sexual abuse, and murderers themselves. Bite marks, lip marks, and rugae patterns are among the forensic techniques employed for identification purposes.

In Hungary, various units such as the Counter Terrorism Centre (TEK), Hungarian National Organisation for Rescue Services (HUNOR), and the Urban Search and Rescue (USAR) team of Hungary (HUSZÁR) strive to be deployed swiftly to provide assistance and protect assets in terror and disaster situations. To adhere to international standards, the Hungarian Victim Identification Service (DVI Hungary) was established in 2018 under the guidance of the National Investigation Bureau of the Hungarian Police. DVI

Hungary aims to create a volunteer-based service with trained professionals, necessary equipment, logistics, and legal authority to be deployed promptly. However, the lack of appropriate equipment, facilities, and software support systems often hinder identification efforts, necessitating investments in infrastructure development.

Our team proposed a method utilizing an intraoral scanner (IOS) to capture mainly the hard palate for human identification. The specificity of forensic characteristics is often criticized because of inappropriate testing or the use of a small subject population. However, conventional statistical sample size estimation does not work here. Furthermore, the total population in the world cannot be investigated. To overcome this concern, we hypothesized that individuals who are as similar as possible (such as identical twins) should be distinguished by a unique method to prove that palate morphology is distinctive. As far as we are concerned, monozygotic (MZ) twin pairs have the highest phenotypic similarity. The question is whether human palate morphology can distinguish between siblings of MZ pairs and whether IOS is reliable enough to detect these minor differences. According to our palatoprint theory, if we can distinguish between two genetically nearly identical individuals, such as identical twins, on the basis of the palate, i.e., phenotype, then we can distinguish between anyone based on palate.

While the utilization of palate and rugae patterns for human identification in forensic practice may not be as commonly established as other methods, there is growing research and literature suggesting their potential value in forensic applications. Recent studies have explored the use of rugae patterns as a unique identifier, offering promising insights into their usefulness for human identification purposes. Thus, further research and advancements in this area may enhance the practicality and reliability of utilizing palate and rugae patterns in forensic practice. However, with the proper scientific evidence and legal regulation, software development, and digital scans, a quick, simple, and easy-to-use human identification method could be developed that would allow us to distinguish twins and sexes based on palate morphology.

1. Introduction

Focusing research on proving uniqueness hinders progress on more important projects and delays addressing key issues like defining "unique" and quantifying certainty. Assumptions of uniqueness in disciplines such as fingerprints and toolmark analysis mask the lack of research data and mislead those deciding on the facts (1). Uniqueness cannot be proven and is not as relevant as believed, as errors arise from guesswork, poor performance, lack of standards, bias, and observer mistakes (1). Forensic science, with its ever-evolving techniques and technologies, constantly seeks to enhance the accuracy and efficiency of human identification processes. One area of interest is the morphology of the palate, which has been studied for centuries. Recent advancements in technology, such as intraoral scanners, offer exciting possibilities for incorporating palate morphology into forensic practice. Intraoral scanners provide detailed and precise 3D images of the oral cavity, allowing for the capture of intricate palate features, including rugae patterns. By utilizing intraoral scanners, forensic experts can potentially compare these patterns to existing databases (if any) or create individualized profiles for accurate identification in various forensic scenarios. This integration of palate morphology analysis with modern technologies exemplifies the ongoing efforts to improve forensic science and strengthen human identification capabilities.

1.1 Morphology of the palate and rugae to establish identity

The anatomy of the palate was first described by Winslow in 1732, nearly 300 years ago (2), followed by the description of rugae by Allen Harris in 1888, approximately 150 years later (3). It is well known that teeth and palatal ridges are stable and identifiable patterns over time (4-11). The literature presents various classifications of rugae (7, 12, 13); however, subjective assessments dominate studies on the shape, size, and orientation of the rugae (5, 14, 15) as well as the shape and depth of the palatal vault (16, 17). In forensic odontology, the pattern of palatal rugae has been analyzed for identification purposes (18), and it has been suggested that there is a significant difference between subjects (19). Orthodontic treatment and tooth extraction may have a partial influence on the pattern of rugae; the first third of the hard palate tends to remain relatively stable, resulting in a constant shape of the rugae and palate height during orthodontic treatment. However, the width undergoes the most significant changes (20, 21). The hard palate is

well protected by the teeth, maxilla, buccal fat pad, lips and **viscerocranium** (22). Since the rugae are protected by several anatomical structures, the rugae remain unaffected for a minimum of seven weeks following severe burns, observed in both deceased individuals and patients (23). Utilizing three-dimensional digitized palates enables precise geometric measurements, facilitating a deeper understanding of morphology and the use of objective methods for measurement (24-26) and the development of an automatic pattern recognition method using artificial intelligence. The superposition of the palatal scans and the calculation of the surface deviation may have eliminated the former approach when identification was made by visual classification of the rugae (12, 27, 28).

1.1.1 Distinguishing the sex in forensic odontology

Previous studies (29-32) have suggested that sex identification can be achieved by examining the palatal and dento-alveolar characteristics, particularly the number and distribution pattern of rugae. However, the process of manually labeling, measuring, and classifying individual rugae is both time-consuming and subjective. The automation of this process also presents a challenge. Limited research has been conducted on sex discrimination using geometric measurements of the palate (33-35), with limited studies conducted using plaster casts (36) or digitized bony palates (34, 37).

1.2 Intraoral scanners

Intraoral scanners (IOS) have fundamentally changed dentistry in recent years. They increase precision and patients' comfort during treatment, regardless of whether they are undergoing quadrant or full mouth rehabilitation (38). Previously, IOSs were mainly used for single-crown restorations (39). Scans made for a single crown rarely included the palate. Nevertheless, the improved speed and accuracy make IOS suitable for long-term or even full-arch prosthetic work (40, 41). IOS is becoming increasingly popular for the preparation of orthodontic appliances (42), for measuring distances on digital models (25), and for orthodontic diagnostics (43). Recently, the reliability of IOS for the preparation of complete dentures has been proposed (44). In addition to the creation of dental restorations, they are also suitable aids for patient education in cases where there is a high degree of tooth wear (45). With complementary equipment, they can also detect caries supporting the conventional diagnosis (46). These applications often or inevitably

involve the palate; therefore, palatal data are continuously being generated. The scans can be exported as open STL files from dedicated software.

Recent data shows (47-49) that the accuracy of intraoral scanners (IOSs) has significantly improved. In 2019 (50), the repeatability (precision) of digital palatal scans varied between 69 and 117 μm , depending on the IOS. However, in 2021 (51) this precision improved to a range of 18-24 μm . There is a growing number of studies on the role of IOSs in human identification (52), or 3D analysis of the dental arches (53). The use of IOSs in disaster victim identification (DVI) would be a significant improvement in the DVI mission. This can provide forensic experts with critical information to identify the victims accurately, particularly in cases where traditional identification methods are not possible or conclusive. Therefore we proposed that IOSs could speed up the identification process in mass disasters and enhance the accuracy and efficiency.

1.3 Forensic identification

In human identification, three primary sets of data are relied upon to establish the identity of a victim. These include fingerprints, deoxyribonucleic acid (DNA) samples, and dental status (54). A successful comparison of these data involves finding a strong correlation between the ante-mortem and post-mortem records.

Forensic odontology plays a crucial role in the field of forensic science, contributing significantly to the identification of individuals through dental evidence. By scrutinizing dental records, X-rays, and analyzing bite marks, forensic odontologists offer valuable insights and assistance in victim identification, particularly in cases where conventional methods may not be available or inconclusive. The distinct characteristics of teeth, such as dental anomalies, restorations, and dental patterns, serve as crucial tools for establishing an individual's identity. Combining the expertise of dentistry and forensic science, forensic odontology facilitates meticulous examinations of dental remains to provide vital information for investigations and legal proceedings.

1.3.1 The challenges of victim identification

To investigate forensic scenes, DVI collects methods and procedures for identifying victims after catastrophes. However, the designation requires international cooperation since natural disasters and terrorist acts do not respect national borders. Therefore, the

DVI protocol is based on the Interpol Methodological Guide (54). Interpol's philosophy is to identify victims in the most efficient way possible through standardized procedures, continuous organization, and training, respecting the rights of mercy, culture, and humanity. A mass disaster is usually caused by an unforeseeable event in which both human and material damage is significant. Due to the increased number of cases, the rapid biodegradation of the residues, the time factor, and the risk of infection play a critical role. Therefore, DVI utilizes modern interdisciplinary forensic science.

Over the past few decades (55), there has been a drastic increase in the occurrence of disasters, resulting in the loss of approximately 1.23 million lives and impacting over 4 billion individuals. Alongside the tragic loss of human life, there has also been substantial damage to property, totaling nearly USD 3000 billion (56).

DVI protocol is also affected by whether the event is closed or open. In closed cases, the identity of the victims are known from a register. For instance, the list of participants was known in the Mermaid shipwreck in Hungary in 2019 (57) or the Ethiopian air disaster in 2019 (58). An open event is when most victims is not registered from an ante-mortem list. There have been several terrorist incidents in recent years where knowing the country of origin and the exact identity of the victims has been a significant challenge for the authorities. Significant cross-border cooperation was required in 2016 in Brussels (59), Nice (60), Berlin (61), in 2017 in Stockholm (62), Barcelona and Cambrils (63), in 2019 in Christchurch, New Zealand (64), and 2020 in Vienna (65). Similarly, in Beirut (66) and in 2021 in Taiwan (67), human error was the leading cause of the tragedy.

In December 2004, a tsunami caused by a 9.1 magnitude seaquake in South-East Asia killed nearly 230 000 people, making it one of the deadliest open-type natural disasters in modern times. Due to the scale of the event, the most extensive international effort (68) was needed to identify the victims in the shortest possible time. The teams are mainly consisted of police officers, forensic pathologists, forensic anthropologists, forensic odontologists, and fingerprint and DNA analysts. In such cases, the following post-mortem data are routinely collected: DNA and fingerprint samples, personal items, detailed dental status, and dental X-rays (69).

The Thai Tsunami Victim Identification-Information Management Center (TTVI-IMC) was established at the site to enhance effectiveness. The collected corpses were compared with ante-mortem data (70). Special refrigerated containers housed 4,280 victims, and

their post-mortem data were recorded (69). Over 15 months, samples from the victims were processed, resulting in the identification of 90.36% of foreign victims (1,847 out of 2,044) and 74.42% of Thai nationals (1,193 out of 1,603). An automated software system categorized the data as probable, proven, possible, insufficient evidence, or excluded for consistency. Forensic dental experts reviewed the results, which were verified by Thai authorities. Once identification was established, death certificates were issued (69). Data collection was challenging due to time constraints and decay at the disaster site. The process was delayed as only two dental experts input data into the computer system. Additionally, the widespread use of smartphones allowed civilians to instantly capture and share images and videos on social media platforms.

The recent earthquake on the Turkey-Syria border in early February 2023, claiming the lives of over 50,000 individuals (71), underscored the critical importance of having comprehensive global identification data during times of disaster.

From the listed examples, it can be seen that rapid victim identification is essential due to the deterioration of the tissue, the risk of epidemic, and the legitimate expectations of relatives. Furthermore, the government of the concerned countries urges the process.

1.3.2 Obstacles in the use of biometric identifiers

Primary biometric identifiers are used in daily practice, but there are many difficulties that forensic experts face in the process of identification.

DNA analysis is a highly accurate and sensitive technique for human identification (72, 73). On the other hand, DNA analysis necessitates access to a laboratory or specialized facilities, involves significant costs, relies on the availability of ante-mortem reference data, and typically takes longer to yield results compared to alternative identification methods. Fingerprints can easily be destroyed by accidents, such as fire or water, or by intentional damage (74). Even minor damage can prevent identification. Moreover, the fingerprint database is not available to the authorities in most cases. Therefore, tooth identification is essential in many disaster situations (75); however, it is time-consuming, is done mainly by manual analogue methods (76), requires ante-mortem radiographs, and the quantitative assignment of probability values of possible matches to information about the restoration position is limited (77).

New biometric identifiers are therefore needed, such as the hand vein pattern (78), iris pattern (79), or rugae pattern (80).

1.3.3 Dental records in forensic

Besides fingerprints and DNA-based identification, more and more identification is being made by dental methods (69). DNA samples are primarily extracted from canines or, if the canines are damaged or missing, the premolars are used for this procedure. According to today's practice, dental data is recorded in Interpol post-mortem form 600 on-site in analog format and digitized afterward. In addition to status recording, two-dimensional photographic documentation and radiographs are used to supplement the identification process. In cases where individuals have insufficiently documented dental treatment and significant changes to their dentition occur after the collection of ante-mortem data, the accuracy of ante-mortem and post-mortem comparisons can be severely compromised. The success of the identification process is heavily influenced by the healthcare administration system in the respective country. A crucial factor is the availability, digitization, standardization, and ease of searchability of citizens' ante-mortem data, both in terms of quality and quantity. A serious difficulty, for example, was that dental ante-mortem data of Indonesian citizens was scarcely available (68).

1.3.4 Identification of twins and their role in forensic sciences

In the majority of cases, DNA base identification proves to be a suitable method with high specificity (81). Nevertheless, the process of identification can present challenges in cases where there is a lack of available databases or when the DNA sequences are highly similar, as observed in monozygotic twins (MZ). The global population of twins is estimated at around 140 million, of which 32 million are identical twins (82). According to the most recent study, the rate of twin pregnancies worldwide has increased by one-third since the 1980s, from 9.1 to 12.0 per 1,000 births, representing about 1.6 million twins per year, with a slight increase for identical twins, at 4 per 1,000 births (82).

The similarity of monozygotic twins makes phenotypic identification difficult (83), and the identification of MZ twins still faces difficulties in human identification (84). MZ twins are very similar in most aspects, so it can be demanding to differentiate them (83). Monozygotic twins do not have identical fingerprints, but they are highly similar (85). It

is important to find a biometric trait that can distinguish twin pair members from each other with greater efficiency.

2. Objectives

2.1 Application of IOS to identify monozygotic twins

1. To determine the repeatability (precision) of palatal scans.
2. To compare the deviation of palatal scans between monozygotic (MZ) siblings to the repeatability.
3. To estimate the probability of distinguishing between MZ siblings by calculating tolerance limits.
4. To estimate the probability of distinguishing between MZ and dizygotic (DZ) twins.
5. To determine the effect of age on the difference between twin siblings.
6. To investigate the possibility that the intraoral scanner is suitable for forensic identification between twins.

2.2 The discriminative potential of palatal geometric analysis for sex discrimination and human identification

We proposed that digital palatal geometry is a good candidate for prescreening for human identification, as an adjunct in forensic dental identification, and as contextual evidence for sex determination investigation.

1. To determine the contribution of the surface morphology (i.e., rugae) to the discriminative potential of the palate.
2. To determine the reliability of digital palatal geometry measurement.
3. To compare the geometry between sexes
4. To estimate the correlation between geometry parameters (height, depth, and width)
5. To determine the potential of palatal geometry for sex prediction.
6. To determine the discriminative potential of palatal geometry for identification.

3. Methods

3.1 Recruited twin population

A total of 201 twin participants, comprising 147 females and 54 males, were included in the study. Triplets were also included in the study, each consisting of one pair of monozygotic (MZ) twins and one dizygotic (DZ) sibling. The zygosity distribution of the pairs was the following: 64 MZ, 33 same-sex DZ (DZSS), and 7 opposite-sex DZ (DZOS).

The twins were between 17 and 74 years (the mean age was 32, with a standard deviation of 14.5 years). The first-born sibling was denoted by the letter A, and the second-born sibling by the letter B. In the case of triplets, the third-born sibling was denoted by letter the C.

3.1.1 Determination of zygosity

All participants received written information about the subsequent measurements, which allowed them to give written informed consent, and were selected from the Hungarian Twin Register (HTR) database (86). The study was carried out under the Declaration of Helsinki. Ethical approval was granted on July 26, 2018 by the National Health Registration and Training Center (approval number: 36699–2/2018/EKU). Zygosity was determined by a standardized questionnaire with nearly 99% accuracy (87, 88). DZ pairs were also included for comparison. DZ twins share approximately 50% of their genetic material, while MZ twins are almost 100% identical regarding their genetics.

The MZ triplet pairs were included in the MZ groups, whereas the DZ ones in the DZ groups. Therefore, one MZ comparison and two DZ comparisons were made within each triplet.

3.2 Application of IOS to identify monozygotic twins

3.2.1 Study subjects

One MZ pair was excluded from the analysis because we failed to make a proper palatal scan. This twin pair has Marfan syndrome with a highly arched palate (89).

199 twin participants, including nine same-sex triplets (147 females and 52 males) were selected from the recruited twin population.

3.2.2 Data acquisition

The palatal area of each subject was scanned with an Emerald® intraoral scanner (Planmeca Oy, Helsinki, Finland, software version Romexis 5.2.1) by a zig-zag scanning pattern (Fig. 1/a), starting from the incisive papilla and finishing at the border of the hard and soft palate. This scan was repeated three times (R1, R2, R3). The same dentist experienced in the Emerald system made all scans, alignment methods, and surface comparisons.

3.2.3 Alignment methods and surface comparison

Each scan was exported as a standard triangulation language (STL) file into the GOM Inspect® software (GOM GmbH, Braunschweig, Germany) for data evaluation and surface comparison. Before the alignments were made, the teeth were cut off from the replicates (Fig. 1/B). Two types of alignments were made using the iterative closest point algorithm (90). First, each scan of the same subject was aligned to each other, and mean surface deviations for the three alignments were calculated (intra-subject deviation, ISD) as shown in Fig. 6/A. Second, the mean deviation between replicates of different siblings within a twin pair was calculated (intra-twin deviation, ITD) as shown in Fig. 6/B, making nine measurements for each pair. The deviation was calculated after surface comparison. The integrated absolute distance and the area of the valid distance between the two surfaces were calculated and transferred to an Excel file, and the mean absolute distance (MAD) was calculated as the ratio of these two parameters to get the absolute mean surface deviation.

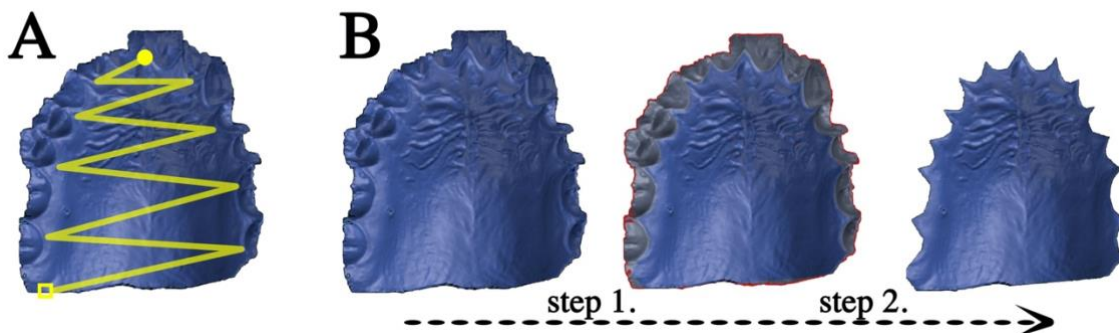


Figure 1. The standard scanning pattern of data acquisition was demonstrated on the upper left side (a). The scan was started by a zig-zag movement from the incisive papilla (yellow

circle) and finished at the border of the hard and soft palate (yellow box). The preparation of the Standard Triangle Language (STL) file was demonstrated on the upper right side (b). Teeth were selected (step 1) and removed (step 2) from the scan, and only the palatal area was kept for alignment and surface comparison.

3.2.3 Statistical analysis

Data in the text and figures are indicated by the mean \pm standard error of the mean (SE). The MAD values showed right-skewed distribution and heteroscedasticity. The variance for ISD and the comparison between ISD and ITD and between mono- and dizygotic ITD were determined by the generalized linear mixed model with gamma distribution and log-link function in SPSS 25 (IBM SPSS Statistics for Windows, Version 24.0). Variances estimated from the model were used to determine a one-sided tolerance interval (upper limit for the ISD and lower limit for the ITD) covering 99% of the population with 95% confidence (alpha level) at least without overlap of the two populations (91). For sample size estimation, the result of a pilot experiment was used involving 22 MZ twin pairs. The mean of ISD was 34 with a standard deviation of 15 μm , and the mean of ITD was 361, with a standard deviation of 93 μm . Tolerance intervals were calculated for a range of sample numbers from 10 to 120, and the result was depicted in Fig. 2. The sample number of 33 was deemed to be eligible to separate the two groups with 99% population coverage with 95% confidence (alpha), and 66 MZ pairs were deemed to be enough to separate them with 99% confidence.

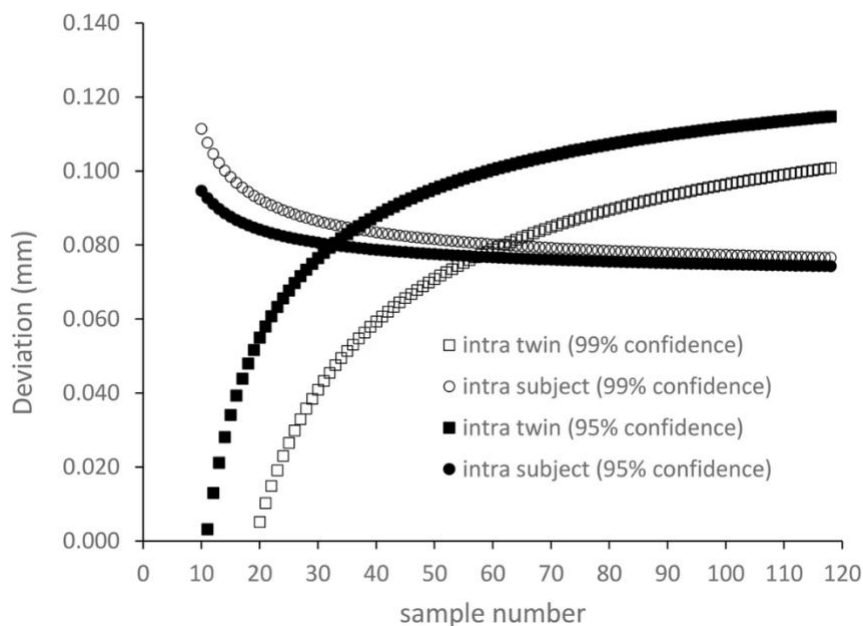


Figure 2. Estimation of sample size for discriminating the intra-subject (box) and the intra-twin (circle) deviation values at the 99% percentile of the population with 95% confidence (filled markers) or with 99% confidence (empty markers)

3.3 The discriminative potential of palatal geometric analysis for sex discrimination and human identification

3.3.1 Study subjects

The opposite-sex twin pairs (7 DZ) and 3 triplets (3 MZ and 6 DZ) were excluded from this study. One same-sex DZ pair was excluded due to a flawed scans. 61 MZ and 26 same-sex DZ twin pairs were selected from the recruited twin population.

3.3.2 The effect of the surface morphology (rugae) on MAD, smoothing the palate

Three replicates of all the remaining subjects (522 scans) were included in the measurement. The scans were imported into the GOM Inspect® 3D mesh processing software. The teeth and the marginal gingiva were digitally removed, generating a palate-only model. The images were further processed by a 3D mesh editing software (Meshmixer, version 3.5, Autodesk Inc., San Rafael, CA, U.S.A.). The palatal rugae surface morphology was removed by the "Sculpt" function, to generate smoothed scans (Fig. 3B).

The superimposition was performed between the three replicates of the twin siblings on the original and smoothed scans by the GOM Inspect® software local best-fit function using an iterative closest point algorithm (90). Finally, a MAD analysis was done, and the software calculated the intra-twin MAD for the original and the smoothed superimposition.

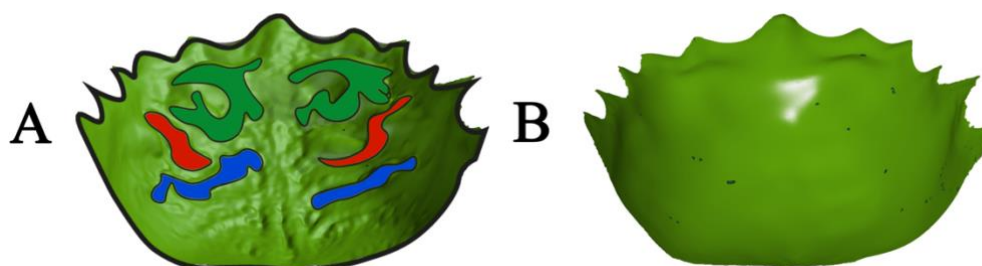


Figure 3. (A) Methods for analyzing the palate-only model. Palatal rugae are depicted in three colors (green, red, and blue) in the original model. (B) The same model is shown after smoothing the rugae.

3.3.3 Geometric measurement of the palate

For the geometric measurement of the palate, an additional 28 twin pairs scans were excluded due to inadequate imaging of the first molar in at least one of the sibling's scans. Therefore, only 42 MZ and 17 DZ for a total of 59 scans could be analyzed.

The scans were imported into GOM Inspect software, and height, depth, and width were measured according to Ferrario et al. (92). Briefly, the Intermolar Line (IML), drawn between the first right (RM) and first left molar's (LM) palatal groove at the level of the gingival margin (Fig. 4A), determined the palatal width. Next, the IML was projected perpendicular to the most anterior point of the incisive papilla (IP), and the intersection point was named Central Point (CP). The line connecting the CP with the IP defined the palatal depth, while the three points (RM, LM, IP) defined the Bottom Horizontal Plane (BHP). Then, a second horizontal plane, the Top Horizontal Plane (THP), parallel to BHP and tangential to the highest point of the palate, was constructed using Chebyshev's best-fit algorithm (Fig. 4B). Finally, the palatal height, the distance between the two planes (THP and BHP) was calculated.

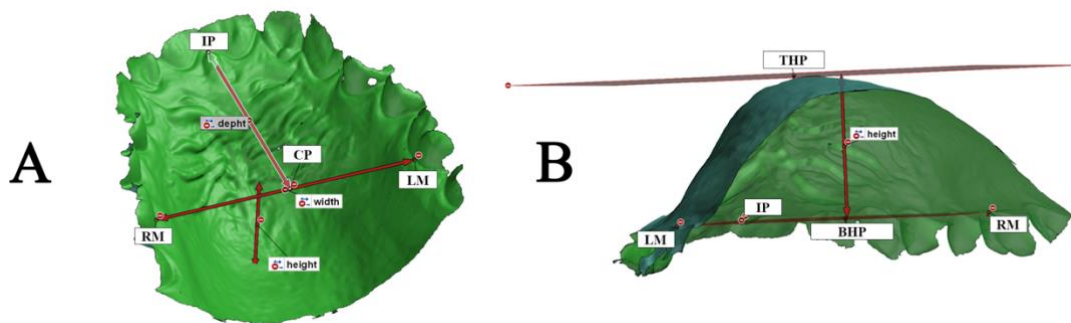


Figure 4. (A) The width and depth measurements were determined using specific points and distances. These points are as follows: Right Molar (RM) representing a point at the gingiva of the right molar, Left Molar (LM) representing a point at the gingiva of the left molar, Incisive Papilla (IP) representing the most anterior point of the incisive papilla, and Central Point (CP). The width measurement is the distance between RM and LM,

while the depth measurement is the distance between IP and CP. Regarding the method for height measurement, it was conducted by defining the horizontal plane (BHP) using the points IP, RM, and LM. The top horizontal plane (THP) was defined as a parallel plane to the horizontal plane positioned at the highest point of the palatal vault. The height measurement refers to the distance between these two planes.

3.3.4 Statistical analysis

The MAD showed a right-skewed distribution in the “Application of IOS to identify monozygotic twins” study, indicating the greater frequency of scan pairs with lower MAD. The data also shows heteroscedasticity (standard deviation is unequal across the range of values), meaning higher MAD has a greater data range (higher standard deviation). Therefore, the MAD was evaluated by the generalized linear mixed model using the log-link function and gamma distribution. From the variables being analyzed, zygosity (MZ, DZ), smoothing (original, smoothed), age (covariant), and their interactions were the fixed effects.

In geometric measurement (height, depth, and width), one scan from the three replicates of each subject was evaluated by two observers to assess the inter-observer variability. The single (ICC (2,1)) and the average rater (ICC (2,2)) absolute agreement and the mean difference between the observers were calculated by the two-way random-effects model (93). The technical error of measurement (TEM) and its relative forms (% TEM) were calculated according to Ulijaszek and Kerr (94).

The male and female palatal width, depth, and height were compared using a linear mixed model. The Pearson correlation coefficients between geometric parameters were calculated for MZ and DZ pairs

Linear discriminant analysis (LDA) created discriminant functions. The discriminant loadings of the height, depth, and width provide information on the relative importance of each variable in determining the sex class. 0.30 is seen as the cut-off between important and less important variables (95). Additionally, two classification equations (i.e., Fisher's linear discriminant functions) were calculated for the female and the male classes. They were used for predictive discriminant analysis. Two classification scores were calculated from the two classification equations for each test case. The

likelihood of the sex of a scan was calculated from the classification score for each case using the Bayesian theorem (96).

A second analysis was performed using a combination algorithm without repeats (the order is not relevant, and no repeats are allowed) in M.S. Excel Visual Basic. The algorithm created 62481 combinations between the 354 scans. Each pair was classified as identical (repeated scans of the same subject), MZ sibling (scan pair of siblings), DZ sibling, or stranger (scan pair of non-relative subjects). The absolute value of the differences between geometric parameters was calculated and square rooted to normalize the distribution (sqrd_height, sqrd_depth, and sqrd_width). Finally, LDA was applied to assess the probability of the classification. All analyses were carried out using IBM SPSS Statistics, Version 27 (Armonk, NY: I.B.M. Corp., U.S.A.). A p-value of less than 0.05 was considered statistically significant.

4. Results

4.1 Application of IOS to identify monozygotic twins

4.1.1 Repeatability (precision) of palatal intraoral scan

With 199 subjects (including all types of twins), the mean absolute distance (MAD) between palatal scans in the intra-subject group (ISD, i.e., repeatability or precision) was $35.3 \mu\text{m} \pm 0.78 \mu\text{m}$. No differences in ISD were observed between monozygotic (MZ) and dizygotic (DZ) twins (36.2 ± 0.9 vs. 34.5 ± 1.2 , $p = 0.271$). The calculated upper tolerance intervals for both types of twins were as follows (Fig. 5),

- $67 \mu\text{m}$ with 99% population coverage and with 95% confidence,
- $68 \mu\text{m}$ with 99% population coverage and with 99% confidence,
- $95 \mu\text{m}$ with 99.999% population coverage and with 99% confidence

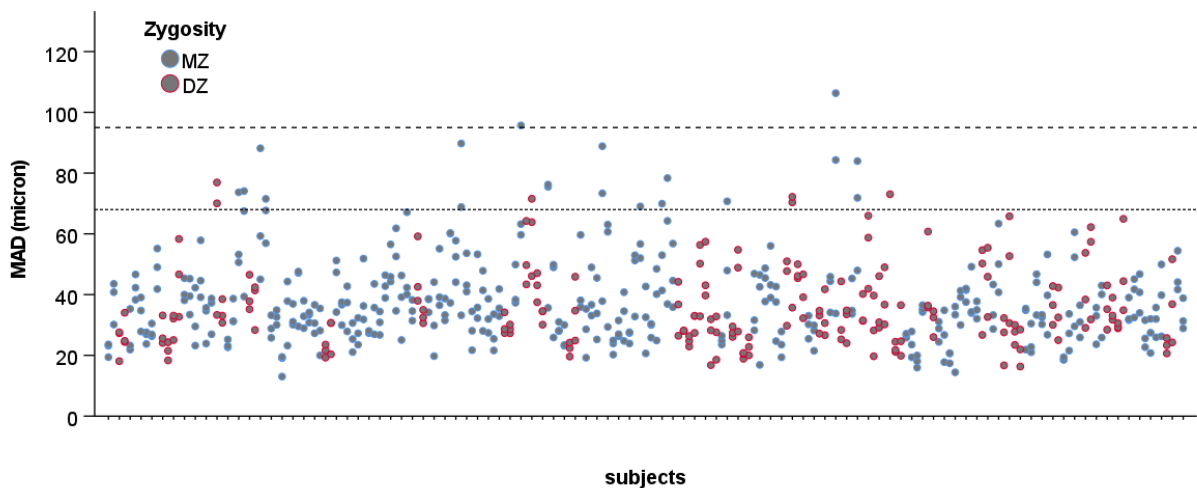


Figure 5. The mean absolute distance (MAD) between scans within a subject (repeatability) of monozygotic (MZ, blue dots) and dizygotic (DZ, red dots) twins. The lower dashed line indicates an upper 99.0% tolerance interval with 99% confidence ($68 \mu\text{m}$). The upper dashed line indicates the upper 99.999% tolerance interval with 99% confidence ($96 \mu\text{m}$).

4.1.2 The deviation of palatal scans between MZ siblings

The superimposition of two scans of the same subject (Fig. 6A) consistently resulted in a smaller MAD than the deviation between two scans between siblings of the same MZ pair, i.e., inter-twin deviation (ITD) (Fig. 6B). The mean ITD of the 64 MZ twins was

significantly higher than the ISD values ($411 \pm 15.2 \mu\text{m}$ vs. $37 \pm 1.1 \mu\text{m}$, $p < 0.001$) (Fig. 6).

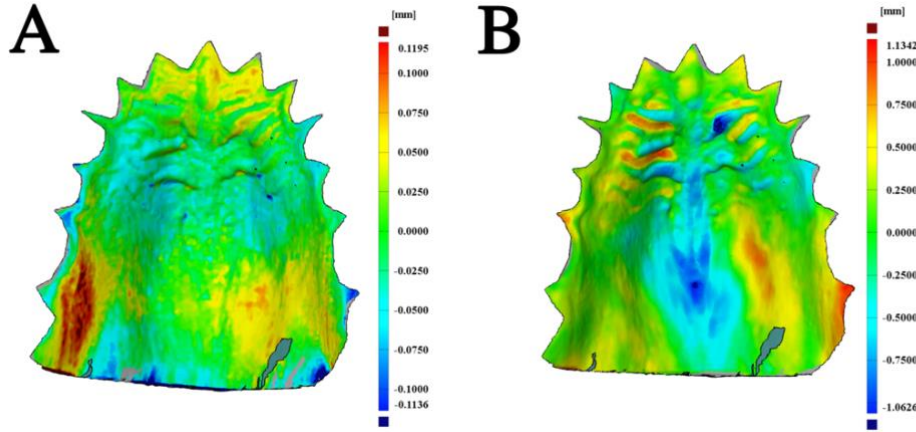


Figure 6. The color-coded surface distance between two aligned scans. Figure A shows the surface comparison of two repeated scans in a monozygotic (MZ) subject, referred to as Intra-Subject Deviation (ISD). Figure B depicts the surface comparison of two scans from siblings in a monozygotic twin pair, known as Intra-Twin Deviation (ITD). In both figures, the color-coded scale bar on the right side indicates the magnitude of distance, specifically the mean absolute distance (MAD), between the aligned surfaces. It should be noted that the scale in figure B is one order of magnitude higher compared to figure A.

4.1.3 The probability of distinguishing between MZ siblings

The calculated lower 99% tolerance limit (with 99% confidence) of the ITD of MZ twins was $147 \mu\text{m}$, and the upper 99% tolerance interval of ISD was $73 \mu\text{m}$ with 99% confidence (Fig. 7).

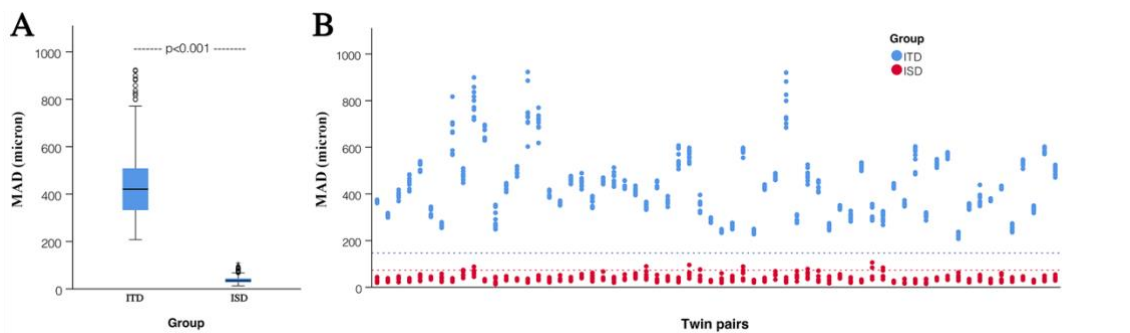


Figure 7. The difference in the mean absolute distance (MAD) between the Intra-Subject Deviation group (ISD) and Intra-Twin Deviation group (ITD). The graphical representation (Figure A) includes the median value (indicated by a horizontal line), the interquartile range (represented by a box), the full range of values without outliers (shown as whiskers), and any outliers (represented by circles). Figure B illustrates the dispersion of individual MAD values. The lower dashed line indicates the upper 99% tolerance interval with 99% confidence (73 μm) for the intra-subject deviation values. On the other hand, the upper dashed line indicates the lower 99% tolerance interval with 99% confidence (138 μm) for the intra-twin deviation values.

4.1.4 The probability of distinguishing between MZ and DZ twins

The mean ITD of MZ twins ($406 \pm 15 \mu\text{m}$) was significantly lower than that of dizygotic same-sex twins (DZSS) ($594 \mu\text{m} \pm 53 \mu\text{m}$, $p < 0.01$) and that of dizygotic same-sex twins (DZOS) ($853 \mu\text{m} \pm 202 \mu\text{m}$, $p < 0.05$). No significant difference was observed between DZSS and DZOS twins (Fig. 8). The tolerance limit was not calculated due to the substantial overlap between data of MZ and DZ populations.

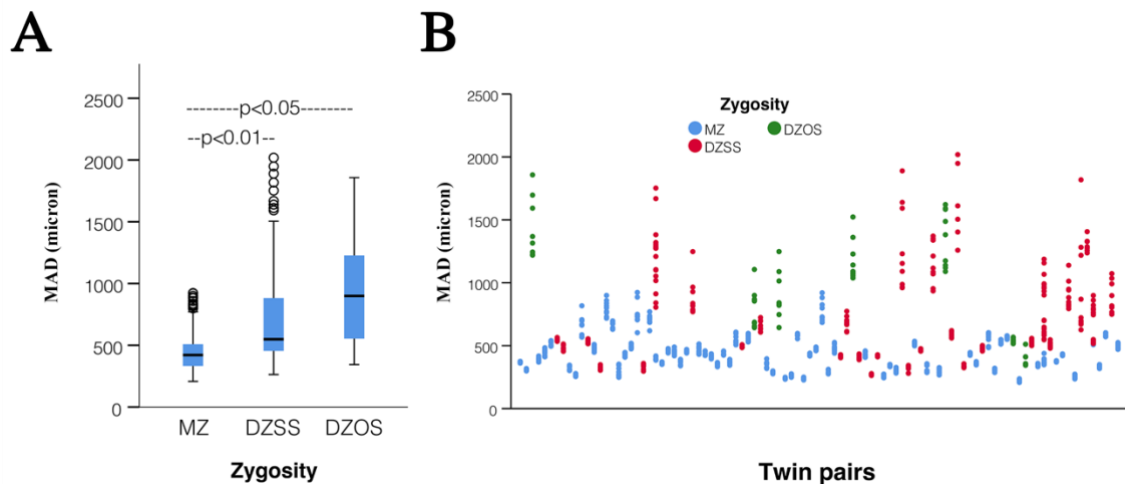


Figure 8. The difference in mean absolute distance (MAD) in the Intra-Twin Deviation group (ITD) between monozygotic (MZ) and dizygotic same- and opposite-sex twins (DZSS and DZOS). The median (horizontal line), interquartile range (box), full range without outlier (whiskers), and the outliers (circles) (A) and dispersion of individual values (B) are shown.

4.1.5 Effect of age on ITD

A weak but significant correlation ($r = 0.3$, $p < 0.05$) was found between the ITD and the subject's age in MZ twins (Fig. 9). From the regression equation ($y = 384 + 3 * \text{age}$), the mean ITD was $430 \mu\text{m}$ at age 17, and it increased by three μm every year.

No correlation was found between ITD and age in DZ twins and between ISD and age in MZ or DZ.

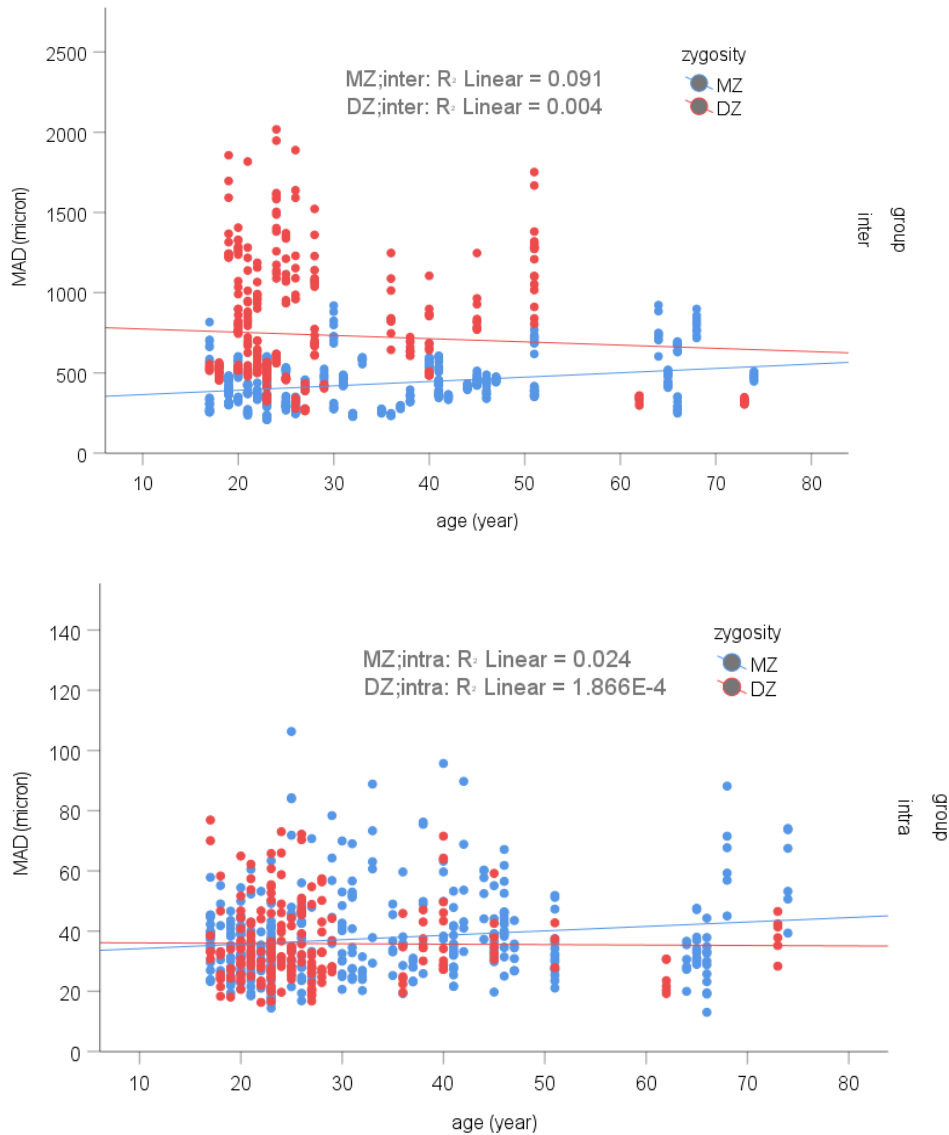


Figure 9. Correlation between age and the mean absolute surface deviation between two scans. The upper panel of the graph represents the deviation between twin siblings, referred to as Intra-Twin Deviation (ITD), while the lower panel represents the deviation

within a single subject, known as Intra-Subject Deviation (ISD). In the graph, blue dots represent monozygotic twins (MZ), and red dots represent dizygotic twins (DZ).

4.2 The discriminative potential of palatal geometric analysis for sex discrimination and human identification

4.2.1 The contribution of the surface morphology to the discriminative potential of the palate.

The ITD MAD of the original scan was not significantly different from the smoothed scan in either MZ (0.430 ± 0.018 mm vs. 0.425 ± 0.022 mm, $p=0.061$) or DZ (0.621 ± 0.058 mm vs. 0.586 ± 0.053 mm, $p=0.284$) (Fig. 10A).

After smoothing, MAD was expected to decrease due to eliminating the "hills and valleys" of the rugae. However, the representative case (Fig. 10B) shows that the MAD did not change significantly because of the shallowness of the rugae.

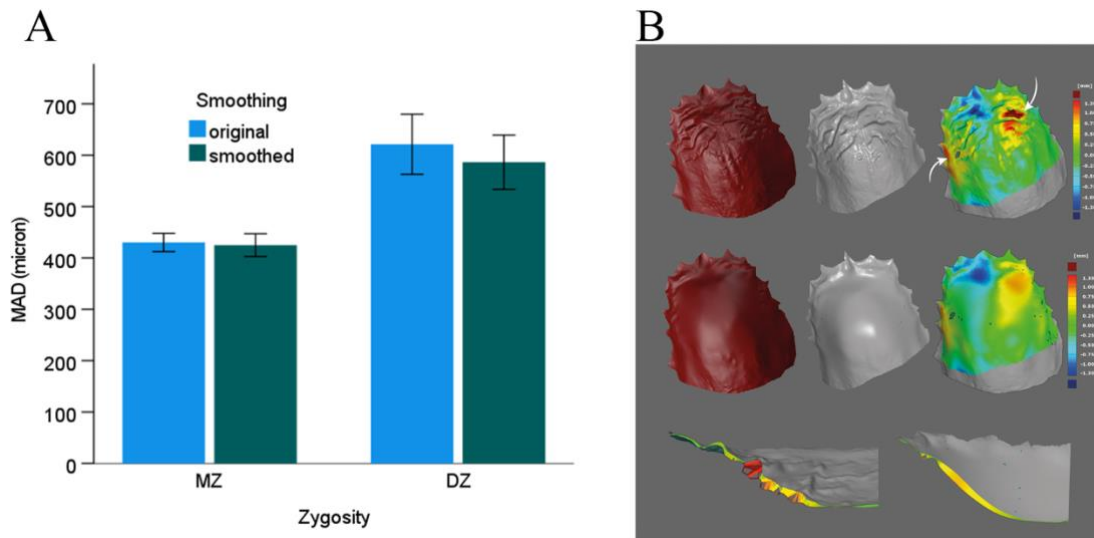


Figure 10. (A) Comparison of the mean absolute distance (MAD) \pm SE (error bars) between original and smoothed scans in monozygotic twin pairs (MZ) and dizygotic twin pairs (DZ). (B) Representative scans of an MZ pair. The first row shows the original scan of sibling A (red) and sibling B (grey). The primary rugae pattern is similar, but some differences can be seen. The white arrow in the original superimposed image (third image) indicates an area with a high distance between the two scans. The second row shows the smoothed scans of the identical twin pair. In their superimposition (third image in the second row), a high deviation area can be seen in the same area as in the original superimposition. It indicates that the distance between scans is primarily caused by geometry. The cross-section of the models (third row) shows that the distance between the two surfaces did not change significantly after smoothing (second image).

4.2.2 Reliability of palatal geometry measurement

The coefficient of variation shows the variability of repeated scans in relation to the mean and is calculated by dividing the standard deviation by the mean. The coefficient of variation was 3.7% for the height, 3.5% for depth, and 1.0% for width, indicating excellent scanning repeatability (high precision).

The ICC was used to quantify the degree of agreement of the measurement between the two observers. For height, depth, and width, the single and average measurements between observers show a high level of agreement (Table 1). However, the statistical analysis revealed that the first observer had a statistically significantly ($p < 0.05$) higher measurement for height than the second observer, the average difference between the two observers was less than 0.1 mm for all measurements. The TEM, measured in mm, expresses the error in anthropometry (the science of measuring the human body) and represents the inter-observer absolute variability of the measurements. % TEM is the relative error calculated by dividing the TEM by the measurement mean. The TEM and % TEM were the lowest for the height and highest for the depth.

TABLE 1 The inter-observer agreement for height, depth, and width

	Absolute agreement (ICC)		Difference between observers			Technical error of measurement	
	single observer (Type ICC 2,1)	average observer (Type ICC 2,2)	mean	SE	p	TEM	%TEM
height (mm)	0.996	0.998	0.07	0.01	0.000	0.10	0.7%
depth (mm)	0.955	0.977	-0.06	0.07	0.380	0.53	1.8%
width (mm)	0.986	0.993	0.04	0.04	0.324	0.31	0.9%

intraclass correlation coefficient (ICC); technical error of measurement (TEM); relative TEM (% TEM)

4.2.3 Comparison of the geometry between sexes

The metric data for height, depth, and width are shown in Table 2. As expected, palatal height and width were significantly higher in males than in females by 2.4 mm and 1.6 mm, respectively. However, the difference in depth proved statistically insignificant.

TABLE 2 Comparison of palatal geometry between sexes

		Valid N	Mean	SE	SD	Minimum	Maximum	Range	p<
height	female	90	15.1	0.16	1.54	11.7	18.5	6.8	0.001
	male	28	17.5	0.42	2.24	14.4	24.1	9.7	
depth	female	90	28.1	0.26	2.48	22.2	34.1	11.9	=0.149
	male	28	29.1	0.37	1.97	25.7	32.8	7.0	
width	female	90	34.0	0.27	2.56	27.0	41.0	14.0	0.05
	male	28	35.6	0.52	2.73	30.3	41.8	11.5	
Standard Error of Mean (SE); Standard Deviation (SD)									

4.2.4 Correlation between geometry parameters

No correlation ($r = 0.13$, $p = 0.164$) was seen between palatal height and palatal depth nor between palatal width and either palatal height ($r = -0.04$, $p = 0.689$) or palatal depth ($r = 0.13$, $p = 0.163$). These results indicated that palatal height, depth, and width are independent variables suitable for LDA.

4.2.5 Linear discriminant analysis for sex prediction

The LDA used to predict the sex classification of an individual produced a function with significant Wilks' Lambda, a measurement of how well a function separates cases into groups (0.66, $p < 0.001$). The data suggest that height has the highest degree of discrimination for sex classification ($r = 0.83$), and width ($r = 0.37$) and depth ($r = 0.24$) have lower degrees of discrimination.

Linear discriminant analysis of the data produced the following two classification formulas, which were then used to test how well these measurements could differentiate between sexes (i.e., predictive classification),

$$Y_{\text{female}} = 6.45 \times \text{height} + 5.56 \times \text{width} + 4.23 \times \text{depth} - 204$$

$$Y_{\text{male}} = 7.35 \times \text{height} + 5.91 \times \text{width} + 4.33 \times \text{depth} - 233$$

The three geometry parameters were inputted into both the female and male equations, and the predicted class was assigned based on whichever equation gave the higher score. Based on the Bayesian theorem, the greater the difference between the two scores, the higher the probability of correct classification (96).

For example, one test subject with a palatal height of 13.9 mm, a palatal depth of 25.1mm, and a palatal width of 34.1mm would yield a female classification score of 182 and a male classification score of 179. Therefore, these calculations would predict females, and the classification was correct in that particular case. In addition, because of the considerable difference between the two scores, the Bayesian probabilities were 0.94 for the female and only 0.06 for the male. The second example (height =13.8, depth 28.0, width 41.0) produced a female score of 232 and a male score of 231. Consequently, the probabilities (female, 0.54; male, 0.46) are close to 50%. Although the predicted memberships were still correct (i.e., female), the prediction probability was significantly lower than in the first example.

When the equations were run on the entire data set using a simple majority ($p > 0.50$) as the predictor, the function correctly classified 74 of the 90 females (sensitivity, 82.2%, specificity, 89.3%) and 25 of the 28 males (sensitivity, 89.3%; specificity, 82.2%).

4.2.6 The discriminant function of geometry parameters for identification

A similar LDA was used to classify repeated scans of the same subject (Y_{identity}), MZ sibling (Y_{MZT}), DZ sibling (Y_{DZT}), and stranger (Y_{stranger}), and it produced significant functions (Wilks' Lambda, 0.955; $p < 0.001$). In all these cases, the data showed that height had the highest discrimination potential (0.63), followed by width (0.62) and depth (0.47). The absolute difference in the geometry parameter between all combinations of scans needed to be calculated. Because the analysis requires normal distribution values, the absolute differences had to be square rooted before input into the following equations.

$$Y_{\text{identity}} = 1.01 \times \text{sqr_height} + 1.00 \times \text{sqr_width} + 1.73 \times \text{sqr_depth} - 2.46$$

$$Y_{\text{MZT}} = 2.25 \times \text{sqr_height} + 2.15 \times \text{sqr_width} + 2.75 \times \text{sqr_depth} - 5.07$$

$$Y_{\text{DZT}} = 2.87 \times \text{sqr_height} + 2.81 \times \text{sqr_width} + 3.20 \times \text{sqr_depth} - 7.02$$

$$Y_{\text{stranger}} = 3.59 \times \text{sqr_height} + 3.57 \times \text{sqr_width} + 3.65 \times \text{sqr_depth} - 9.23$$

Again, the classification was based on whichever equation gave the highest score. The function correctly classified scans of the same individuals by (91.2% sensitivity and 97.8%). Due to the similarity of the Y_{MZT} and Y_{DZT} formulas, the groups were combined. The "twin classification" was determined with 68.5% sensitivity and 61.9% specificity.

TABLE 3 Identification based on palatal geometry						
		Predicted Group Membership				Total
	Original class	identical	MZ pair	DZ pair	stranger	
True	identity	323	21	3	7	354
	MZ sibling	76	217	58	27	378
	DZ sibling	19	44	45	45	153
	stranger	1291	12653	10922	36730	61596
%	Identity	91.2	5.9	0.8	2.0	100
	MZ sibling	20.1	57.4	15.3	7.1	100
	DZ sibling	12.4	28.8	29.4	29.4	100
	stranger	2.1	20.5	17.7	59.6	100
True	MZ + DZ	95	364		72	531
%	MZ + DZ	17.9	68.5		13.6	100
monozygotic twins (MZ); dizygotic twins (DZ)						

5. Discussion

The clinical relevance of intraoral scanners in identifying monozygotic twins is significant. By superimposing intraoral scans of the palate, it becomes possible to confidently distinguish between monozygotic twin siblings. This unique capability extends the potential for palatal scan uniqueness to the entire human population, presenting a valuable tool for identification purposes. Furthermore, intraoral scanners facilitate quick and straightforward acquisition of ante- and post-mortem data, enhancing efficiency in forensic investigations.

Palatal geometric analysis offers discriminative potential not only for twin identification but also for sex discrimination and human identification. With the increasing availability of 3D data from intraoral scanners, distinctive identification features can be extracted from palatal geometry. This technique holds promise as a valuable triage tool, reducing the number of potential matches and streamlining the identification process. Additionally, palatal geometry can provide contextual evidence to support sex determination, augmenting the overall accuracy and reliability of forensic assessments.

5.1 Application of intraoral scanner to identify monozygotic twins

The precision of the measurements was evaluated by determining the absolute surface distance between scans of the same individuals. An ISD of 35.3 μm is better than what was found in previous studies (50, 97), providing a range between 55 and 117 μm . Our goal was to calculate the upper tolerance limit of ISD with 99% coverage of the population and 95% confidence. The upper boundary signifies that 99 out of 100 measurements are expected to fall below this level with 95% certainty. With a relatively large sample size and highly precise palatal scans, we were able to increase the population coverage to 99.999% and the confidence to 99%. This implies that out of 100,000 ISD measurements, 99,999 will be less than 95 μm . This assessment was conducted with three replicates. In the context of forensic science or forensic identification, it is recommended to have a minimum of two scans for control purposes. If the measured deviation value exceeds 95 μm after aligning the two scans, it is advised to perform a new scan. Based on our experience, a palatal scan can be completed within 18 to 22 s, with an additional minute required for alignment.

Among the investigated 64 MZ pairs, the smallest difference between two scans obtained from different siblings of the same MZ pair was 208 μm . Conversely, the highest difference within the same individual was 106 μm . There was no overlap between the two sets of data. By calculating tolerance intervals, we can estimate values for the entire population. Based on our findings, the inter-twin deviation (ITD) values can be distinguished from the intra-subject deviation (ISD) values with 99% confidence at a 99% tolerance limit. The lower limit of ITD (138 μm) and the upper limit of ISD (73 μm) do not intersect. These results indicate that despite having nearly identical DNA sequences, there are differences in the palate morphology between members of MZ twin pairs. The intraoral scans captured with the Emerald intraoral scanner on palatal soft tissues reliably differentiate between individuals within MZ twin pairs. According to our results, if we compare two unidentified intraoral scans and the measured deviation value exceeds 138 μm , we can be 99% certain that these scans do not belong to the same individual, even if that individual has an MZ twin sibling.

The utilization of palatal scans in forensic odontology offers notable benefits. Unlike teeth, which undergo continuous changes due to dental treatments, the palatal area remains relatively stable throughout an individual's life. It is less vulnerable to external impact than other external surface structures, such as fingerprints (22, 23). The 3D evaluation of landmarks of the palatal rugae showed no significant changes over 2 years (11). Notably, the horizontal dimension of the maxillary arch was not different from 13 to 45 years of age (98). It can be assumed that palatal morphology remains unchanged over time. However, our findings indicate that the difference between siblings within a monozygotic (MZ) pair slightly increases with age. This observation can be explained with different epigenetic changes evolving in MZ twins as they grow older (99). Over 50 years, the difference between two MZ twins increases by about 150 μm on average, and it increasingly approaches the mean deviation between two DZ twins. The increased deviation may be due to the involution of the gingiva after tooth loss. The higher deviation favors the accuracy of identification. The superimposition of the palate could be a reliable method for identifying a person, which was suggested in a previous study (11) as well. However, the method may have some limitations. Some orthodontic treatments, such as the rapid maxillary expansion of the palate, could distort its morphology (100). Sparse data suggest that distances between the palatal rugae may change after graft harvesting

(101). Currently, there is a lack of information regarding the post-mortem laceration of the palate following drowning, the regeneration of its pattern after graft harvesting for periodontal surgery, and the potential alterations caused by tissue atrophy during aging and tooth loss. As a result, it is crucial for future studies to address these fundamental inquiries and conduct investigations into these areas.

Another limitation of our innovative approach is the absence of an accuracy study that evaluates palatal scans using different intraoral scanners (IOSs). In two clinical studies, a conventional polyvinyl siloxane impression was used as the reference model. When compared to the reference model, the trueness of the palatal area scanned with the Trios 3 scanner was found to be 80.5 μm (24). In an earlier study (97) that utilized a similar reference impression and IOS, the trueness of the palate was measured at 130.5 μm . These findings suggest an enhancement in the accuracy of scanners over time. The trueness value of a conventional impression reference model may be distorted. However, in a cadaver scenario, this error can be eliminated by directly scanning the dislocated maxilla using a highly accurate industrial scanner to obtain a reference model (50). It has been the only study so far where the accuracy of the palate scan was evaluated using the Emerald scanner. The trueness and precision were 150.6 μm and 87.1 μm , respectively. However, only the teeth were aligned before the deviation in the palatal region was determined. It is a rational assumption that if a region other than the one measured is aligned, then the best-fit alignment would not be optimized for that region. Alignment at the palatal region instead of the teeth may explain the higher precision (35 μm) in our study.

The trueness of 150 μm measured in the cadaver study (50) is much lower than the mean ITD value (411 μm) of MZ twins in our study and is very close to the lower 99% tolerance limit of the ITD of MZ twins (147 μm). Introducing a different scanner than the one used in the identification process for a previously scanned patient can lead to additional errors. It is important to note that these errors are additive at the variance level, resulting in a slightly lower overall accuracy compared to the sum of the trueness values. Furthermore, a previous study (50) demonstrated that contrary to the conventional impression, all investigated IOSs had positive deviation values, suggesting that the deviation from the true value was in the same direction, which may further decrease the discrepancy between scanners. The feasibility of automated human identification will increase with the

widespread adoption of digital samples, and it is likely that the accuracy of intraoral scanners (IOSs) will also significantly improve by that time. Additionally, in our study, we considered monozygotic (MZ) twins to be the most similar individuals, expecting greater variation among non-twin individuals.

5.2 The discriminative potential of palatal geometric analysis for sex discrimination and human identification

The study observed no notable distinction in intra-twin mean absolute deviation (MAD) between the original and smoothed scans. It is worth mentioning that the iterative closest point algorithm is specifically designed to identify the most optimal comparison by minimizing the distance between a maximum number of points. Hence, the software does not focus on comparing identical structures (90, 102, 103). Despite our initial expectation that the smoothed scans would result in a smaller mean absolute deviation (MAD), this hypothesis was not supported by the findings. This can be attributed to the fact that the variation in surface morphology adds relatively little distance compared to the overall palatal distance. As a result, the alignment method's inherent characteristics contribute only minimally to the MAD, with surface morphology (specifically the rugae) having a more significant impact on morphological comparison. Visual examination of the rugae in MZ twins confirms that they are similar but not identical. Therefore, while geometry primarily influences surface alignment, the rugae play a role in distinguishing between twin pairs when considering morphological comparison. However, these results indicate that the palate's geometry may have the potential to reduce the number of potential candidates, although no correlation was observed between the three palatal parameters, suggesting limited suitability for multivariate discriminant analysis in this study.

Having knowledge of the probable sex of an unidentified individual based on palatal morphology has the potential to significantly reduce 3D database searches by nearly 50%. In this study, the linear discriminant analysis conducted on the Central European Caucasian population achieved an 84% accurate prediction of sex, which can be particularly valuable when other anthropological data is unavailable. Furthermore, in cases where there is a greater distinction in the calculation of scores between males and females, the probability of correct classification would be even higher. Although previous sex classification criteria using rugae pattern, teeth size, teeth morphology (29, 31, 104),

and complex craniometry (105) have been proposed, the method used here is far simpler, using three palatal landmarks. It also has the potential for an Artificial Intelligence algorithm to perform the entire analysis. While previous studies have provided some evidence to support the idea that palatal characteristics can be utilized for individual differentiation, they have generally yielded lower levels of prediction. Our study indicates that this lower prediction level may be attributed to the fact that none of these previous studies took into account the measurement of height, which has been demonstrated to possess the greatest potential for distinguishing both sex and identity. Additionally, an advantage of employing the suggested linear parameters is that they can also be measured from a skull specimen, thereby expanding the applicability of the method to skeletal remains.

5.2.1 Ethnicity and Palatal Metrics

One of the limitations of the current study was that linear discriminant analysis was performed on a homogenous Caucasian Central European population and has not been adjusted for ethnic differences. A study of a mixed male/female Chinese population (97) showed a similar average height to Caucasian Central European (16.6 mm vs. 16.3 mm), but the width was higher (38.0 mm vs. 34.8 mm) than the mixed male/female Caucasian Central European average. A Lebanese study showed that the width difference between males and females was 1.5 mm (31) which compared well to our study (1.6 mm). Previous anthropological research on the ethnic variations in palatal measurements is limited and has produced conflicting findings. One such study focused on skeletal palatal geometry and achieved a 66% successful discrimination rate among three American racial groups (Indian, Afro-Americans, and Euro-Americans) (106). At the same time, the width and depth of the palate were a successful discriminator between American blacks and whites by 83% success (107). The studies indicate that palatal width provides the highest level of discrimination among ethnicities. However, further soft tissue scans of diverse ethnic populations are required to validate the use of automated geometry measurement as an ethnic discriminator.

5.2.2 Use of Geometric Measurement for Human Identification

The technique of superimposing two palatal scans and comparing their morphology can be used to aid in identity verification and eliminate false-positive cases by utilizing intraoral scans (108). Nevertheless, performing such computations on a large-scale database can be computationally demanding. To address this issue, conducting a preliminary assessment by comparing geometric parameters can substantially reduce the dataset and narrow down potential candidate pairs. The geometric comparisons of oral scans from identical subjects showed excellent sensitivity (91.2%) and specificity (97.8%), indicating precise classification. Additionally, the study confirmed that the geometric analysis of twin pairs produced results that were intermediate, lying between inclusion and exclusion. The variance observed in the DZ pairs was slightly higher than that in the MZ pairs.

The study also identified certain limitations of the technique, including challenges encountered in cases where the first upper molars were missing. Moreover, it was observed that 16% of the subjects had missing molars, aligning well with the population data obtained from Odontosearch (<http://www.odontosearch.com/en/3.2/index.html>) (77). The average age of the participants was 32 years, ranging from 17 to 74 years. Most of the discarded scans (90%) were from older individuals. In the future, it may be possible to digitally overlay a horizontal plane on the edentulous ridge to simulate height measurement, which is a highly discriminative parameter. Another aspect to consider is the effect of gingival recession on the RM and LM landmarks. In cases of significant recession, the cemento-enamel boundary can be used as an alternative. However, this approach may be limited when prosthetic restorations obstruct the visualization of these landmarks. Additionally, it is important to note that scans for small restorations may not capture the entire arch. Due to the enhanced accuracy and efficiency of intraoral scanners (IOS) (109-112), a greater number of comprehensive scans are now being conducted to enhance the quality of bite registration data. (113).

5.2.3 Our advances in Palatoprint concept

A decision flow chart with probability values was devised to assist in the process of human identification within forensic odontology (Fig. 11). This chart outlines the recommended workflow for identification. The initial step involves identifying potential pairs based on palatal dimensions. Subsequently, a 3D whole surface superimposition can be employed to validate the results and eliminate false positive cases. If no identity is established, the potential relatedness between individuals can be determined. In the absence of any relatedness, the ethnic group can be inferred, followed by sex identification. While these preliminary tests allow investigators to narrow down the range of possibilities, they do not provide definitive confirmation of identity. Nonetheless, the predictions regarding sex, race, and relatedness offer valuable leads to law enforcement, particularly in cases involving disasters, in contrast to relying solely on a single match/no-match outcome based on dental records and previous dental treatments (114). It should be noted that dental conditions are subject to constant treatment, decay, and wear, which can lead to inconsistencies between ante-mortem and post-mortem data. The comprehensive analysis of dental status requires the expertise of a dental professional (114, 115), as no automated algorithm is currently available.

*Decision flow chart with probability values
for human identification in forensic odontology*

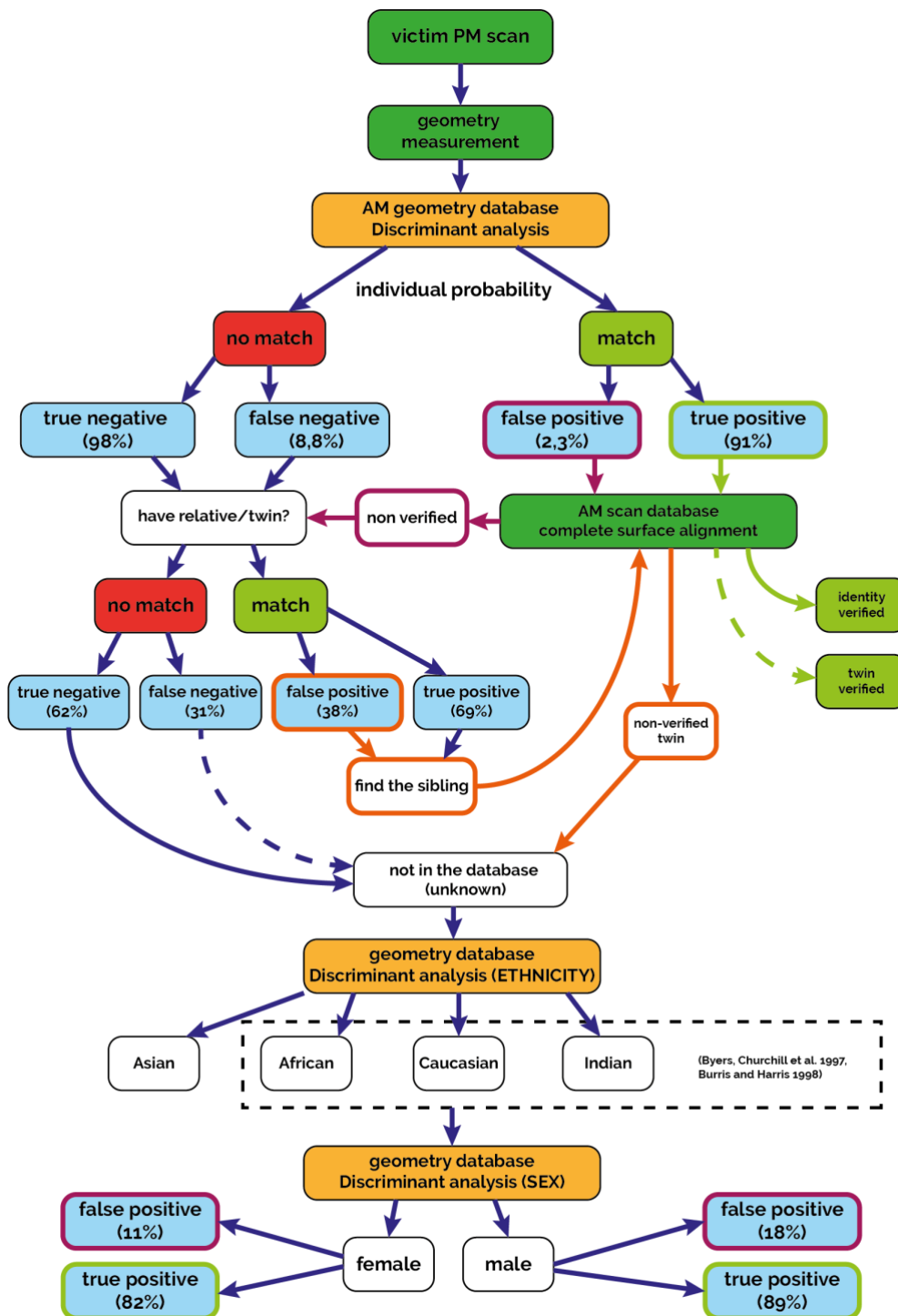


Figure 11. The percentage in the brackets indicates the rate of true negative, false negative, true positive, and false-positive calculated in this study. According to the literature (106, 107), geometry can be used for ethnicity prediction.

6. Conclusions

6.1 Application of intraoral scanner to identify monozygotic twins

- Monozygotic twin siblings can be distinguished from each other with high confidence by the superimposition of intraoral scans of the palate. Therefore, identical twin discrimination implies palatal scan uniqueness for the whole human population.
- Ante- and post-mortem data acquisition by IOS is quick and easy.
- The 3D superimposition is highly reliable; however, searching in big data might not be fast enough. Therefore, further data preprocessing by finding the unique feature on the palatal scan is essential.

6.2 The discriminative potential of palatal geometric analysis for sex discrimination and human identification

- Palatal geometrics possesses unique identification features.
- In addition, as the use of IOSs increases, the availability of 3D data will increase, and this technique could be a valuable triage tool by reducing the possible limiting matches.
- Furthermore, palatal geometry could serve as additional contextual evidence to corroborate other supporting data in sex determination

7. Summary

Objectives: We aimed to develop a human identification system based on an intraoral palatal scan. The first study aimed to compare the palatal scan repeatability to the difference between almost identical twin siblings. The second study aimed to evaluate the discrimination potential of palatal geometric analysis to distinguish individuals, twin siblings, and strangers. Additionally, sex discrimination potential was also assessed.

Methods: Only twins were recruited in our study. In the first study, the palatal surface of 64 MZ twins and 33 same-sex dizygotic (DZ) twins (DZSS) and 7 opposite-sex dizygotic twins (DZOS) were scanned three times with Emerald intraoral scanner. The mean absolute distance between scan surfaces of the same subject (intra-subject deviation, ISD) and between scans of the two siblings within a twin pair (intra-twin deviation, ITD) was measured. The palates of 64 MZ and 39 DZ twins were selected in the second study. Digital smoothing was used to remove the rugae from the 3D palatal scan, and palatal geometric parameters (height, depth, and width) were measured.

Results: The mean ISD of the palatal scan was $35.3 \mu\text{m} \pm 0.78 \mu\text{m}$. The calculated upper tolerance limit was $95 \mu\text{m}$. The mean ITD of MZ twins ($406 \mu\text{m} \pm 15 \mu\text{m}$) was significantly ($p < 0.001$) higher than the ISD, and it was significantly lower than the ITD of DZSS twins ($594 \mu\text{m} \pm 53 \mu\text{m}$, $p < 0.01$) and the ITD of DZOS twins ($853 \mu\text{m} \pm 202 \mu\text{m}$, $p < 0.05$). The ITD of the smoothed palate did not significantly differ from the original one either in MZ ($0.425 \pm 0.022\text{mm}$ vs. $0.430 \pm 0.018\text{mm}$, $p = 0.061$) or DZ ($0.586 \pm 0.053\text{mm}$ vs. $0.621 \pm 0.058\text{mm}$, $p = 0.284$). By combining the height, depth, and width into a discriminative function, the sex correctly correlated 83.9% of the time, identity by 91.2% sensitivity, and twinning by 68.5%.

Conclusion: Palatal intraoral scans demonstrate excellent reproducibility, allowing for differentiation between monozygotic (MZ) twins despite their nearly identical DNA. This finding suggests the potential value of this method in forensic odontology. The variation observed in the 3D palatal models of twin siblings primarily arises from differences in palate geometry. Considering the relatively faster computation time, geometric comparison alone can serve as a supplementary measure to narrow down potential matches in dental 3D databases for determining sex and identity, particularly when other evidence is lacking.

8. References

1. Page M, Taylor J, Blenkin M. Uniqueness in the forensic identification sciences-
-fact or fiction? *Forensic science international*. 2011;206(1-3):12-8.
2. Winslow JB. *Exposition anatomique de la structure du corps humain par JacquesBénigne Winslow: éditeur non identifié; 1732.*
3. Allen H. The Palatal Rugae in Man. *Proceedings of the Academy of Natural Sciences of Philadelphia*. 1888;40:254-72.
4. Azab SMS, Magdy R, Sharaf El Deen MA. Patterns of palatal rugae in the adult Egyptian population. *Egyptian Journal of Forensic Sciences*. 2016;6(2):78-83.
5. Chong JA, Syed Mohamed AMF, Marizan Nor M, Pau A. The Heritability of Palatal Rugae Morphology Among Siblings*†. *Journal of Forensic Sciences*. 2020;65(6):2000-7.
6. Chong JA, Mohamed AMFS, Pau A. Morphological patterns of the palatal rugae: A review. *Journal of Oral Biosciences*. 2020;62(3):249-59.
7. Kapali S, Townsend G, Richards L, Parish T. Palatal rugae patterns in Australian Aborigines and Caucasians. *Australian Dental Journal*. 1997;42(2):129-33.
8. Kommalapati RK, Katuri D, Kattappagari KK, Kantheti LPC, Murakonda RB, Poosarla CS, et al. Systematic Analysis of Palatal Rugae Pattern for Use in Human Identification between Two Different Populations. *Iranian journal of public health*. 2017;46(5):602-7.
9. Limson KS, Julian R. Computerized recording of the palatal rugae pattern and an evaluation of its application in forensic identification. *The Journal of forensic odonto-stomatology*. 2004;22(1):1-4.
10. Taneva E, Evans C, Viana G. 3D Evaluation of Palatal Rugae in Identical Twins. *Case Rep Dent*. 2017;2017:2648312.
11. Taneva ED, Johnson A, Viana G, Evans CA. 3D evaluation of palatal rugae for human identification using digital study models. *Journal of forensic dental sciences*. 2015;7(3):244-52.
12. Lysell L. Plicae palatinae transversae and papilla incisiva in man; a morphologic and genetic study. *Acta Odontol Scand*. 1955;13(Suppl. 18):5-137.
13. Thomas CJ, Kotze TJ. The palatal ruga pattern in six southern African human populations, part I: A description of the populations and a method for its investigation.

The Journal of the Dental Association of South Africa = Die Tydskrif van die Tandheelkundige Vereniging van Suid-Afrika. 1983;38(9):547-53.

14. Gupta V, Kaur A. Palatal rugoscopy as an adjunct for sex determination in forensic odontology (Sri Ganganagar population): A cross-sectional study of 100 subjects. *J Oral Maxillofac Pathol.* 2021;25(3):556.

15. Smitha T, Vaswani V, Deepak V, Sheethal HS, Hema KN, Jain VK. Reliability of palatal rugae patterns in individual identification. *J Oral Maxillofac Pathol.* 2021;25(3):555.

16. Mohammad A, Korlakunte PR. Gender identification and morphologic classification of tooth, arch and palatal forms in Saudi population. *J Pharm Bioallied Sci.* 2015;7(Suppl 2):S486-90.

17. Maria CM, Silva AMTd, Busanello-Stella AR, Bolzan GdP, Berwig LC. Avaliação da profundidade do palato duro: correlação entre método quantitativo e qualitativo. *Revista CEFAC.* 2013;15.

18. Lima de Castro-Espicalsky T, Freitas P, Ribeiro Tinoco RL, Calmon M, Daruge Júnior E, Rossi AC. Human identification by the analysis of palatal rugae printed in complete dentures. *The Journal of forensic odonto-stomatology.* 2020;38(2):57-62.

19. Bailey LT, Esmailnejad A, Almeida MA. Stability of the palatal rugae as landmarks for analysis of dental casts in extraction and nonextraction cases. *Angle Orthod.* 1996;66(1):73-8.

20. Ali B, Shaikh A, Fida M. Stability of Palatal Rugae as a Forensic Marker in Orthodontically Treated Cases. *J Forensic Sci.* 2016;61(5):1351-5.

21. Kinzinger GSM, Lisson JA, Buschhoff C, Hourfar J. Age-dependent effects on palate volume and morphology during orthodontic RME treatment. *Clinical Oral Investigations.* 2023;27(6):2641-52.

22. Jain A, Chowdhary R. Palatal rugae and their role in forensic odontology. *J Investig Clin Dent.* 2014;5(3):171-8.

23. Muthusubramanian M, Limson KS, Julian R. Analysis of rugae in burn victims and cadavers to simulate rugae identification in cases of incineration and decomposition. *J Forensic Odontostomatol.* 2005;23(1):26-9.

24. Zhongpeng Y, Tianmin X, Ruoping J. Deviations in palatal region between indirect and direct digital models: an in vivo study. *BMC Oral Health.* 2019;19(1):66.

25. Rajshekar M, Julian R, Williams AM, Tennant M, Forrest A, Walsh LJ, et al. The reliability and validity of measurements of human dental casts made by an intra-oral 3D scanner, with conventional hand-held digital callipers as the comparison measure. *Forensic Sci Int.* 2017;278:198-204.
26. Paoloni V, Fusaroli D, Marino L, Mucedero M, Cozza P. Palatal vault morphometric analysis of the effects of two early orthodontic treatments in anterior open bite growing subjects: a controlled clinical study. *BMC Oral Health.* 2021;21(1):514.
27. Winsløw JB. *Exposition anatomique de la structure du corps humain: Desprez, Desessartz; 1732.*
28. Poojya R, Shruthi CS, Rajashekar VM, Kaimal A. Palatal Rugae Patterns in Edentulous Cases, Are They A Reliable Forensic Marker? *International journal of biomedical science : IJBS.* 2015;11(3):109-12.
29. Saraf A, Bedia S, Indurkar A, Degwekar S, Bhowate R. Rugae patterns as an adjunct to sex differentiation in forensic identification. *J Forensic Odontostomatol.* 2011;29(1):14-9.
30. Gautam N, Patil SG, Krishna RG, Agastya H, Mushtaq L, Kumar KV. Association of Palatal Rugae Pattern in Gender Identification: An Exploratory Study. *J Contemp Dent Pract.* 2017;18(6):470-3.
31. Saadeh M, Ghafari JG, Haddad RV, Ayoub F. Sex prediction from morphometric palatal rugae measures. *The Journal of forensic odonto-stomatology.* 2017;35(1):9-20.
32. Pakshir F, Ajami S, Pakshir HR, Malekzadeh AR. Characteristics of Palatal Rugae Patterns as a Potential Tool for Sex Discrimination in a Sample of Iranian Children. *J Dent (Shiraz).* 2019;20(1):1-9.
33. Sumati, Patnaik V, A P. Determination of sex from hard palate by discriminant function analysis. *International Journal of Basic and Applied Medical Sciences.* 2012;2(3):8.
34. Chovalopoulou ME, Valakos ED, Manolis SK. Sex determination by three-dimensional geometric morphometrics of the palate and cranial base. *Anthropol Anz.* 2013;70(4):407-25.
35. Velezmoro-Montes Dds MYW, Suárez-Ponce Dds MPDG, Escalante-Flórez Dds KJ. Sexual Dimorphism Via Palatal Vault Morphometric Analysis on A Sample Peruvian Population. *Odovtos - International Journal of Dental Sciences.* 2019:217-25.

36. Mankapure PK, Barpande SR, Bhavthankar JD. Evaluation of sexual dimorphism in arch depth and palatal depth in 500 young adults of Marathwada region, India. *Journal of forensic dental sciences*. 2017;9(3):153-6.
37. Ajanovic Z, Dervisevic L, Dervisevic A, Sarac-Hadzihalilovic A, Dervisevic E, Biscević Tokic J, et al. Sex prediction by geometric morphometric analysis of the hard palate. *Eur Rev Med Pharmacol Sci*. 2022;26(17):6057-64.
38. Siqueira R, Galli M, Chen Z, Mendonça G, Meirelles L, Wang HL, et al. Intraoral scanning reduces procedure time and improves patient comfort in fixed prosthodontics and implant dentistry: a systematic review. *Clin Oral Investig*. 2021;25(12):6517-31.
39. Tsirogiannis P, Reissmann DR, Heydecke G. Evaluation of the marginal fit of single-unit, complete-coverage ceramic restorations fabricated after digital and conventional impressions: A systematic review and meta-analysis. *The Journal of prosthetic dentistry*. 2016.
40. Cappare P, Sannino G, Minoli M, Montemezzi P, Ferrini F. Conventional versus Digital Impressions for Full Arch Screw-Retained Maxillary Rehabilitations: A Randomized Clinical Trial. *International journal of environmental research and public health*. 2019;16(5):829.
41. Wulfman C, Naveau A, Rignon-Bret C. Digital scanning for complete-arch implant-supported restorations: A systematic review. *The Journal of prosthetic dentistry*. 2020;124(2):161-7.
42. Taneva E, Evans C, Kusnoto B. 3D Scanning, Imaging, and Printing in Orthodontics. 2015.
43. Martin CB, Chalmers EV, McIntyre GT, Cochrane H, Mossey PA. Orthodontic scanners: what's available? *J Orthod*. 2015;42(2):136-43.
44. Chebib N, Kalberer N, Srinivasan M, Maniewicz S, Perneger T, Müller F. Edentulous jaw impression techniques: An in vivo comparison of trueness. *The Journal of prosthetic dentistry*. 2019;121(4):623-30.
45. Mitirattanakul S, Neoh SP, Chalarmchaichaloenkit J, Limthanabodi C, Trerayapiwat C, Pipatpajong N, et al. Accuracy of the Intraoral Scanner for Detection of Tooth Wear. *Int Dent J*. 2022.

46. Michou S, Vannahme C, Bakhshandeh A, Ekstrand KR, Benetti AR. Intraoral scanner featuring transillumination for proximal caries detection. An in vitro validation study on permanent posterior teeth. *J Dent.* 2022;116:103841.
47. Ashraf Y, Abo El Fadl A, Hamdy A, Ebeid K. Effect of different intraoral scanners and scanbody splinting on accuracy of scanning implant-supported full arch fixed prosthesis. *Journal of esthetic and restorative dentistry : official publication of the American Academy of Esthetic Dentistry [et al].* 2023.
48. Piedra-Cascón W, Adhikari RR, Özcan M, Krishnamurthy VR, Revilla-León M, Gallas-Torreira M. Accuracy assessment (trueness and precision) of a confocal based intraoral scanner under twelve different ambient lighting conditions. *Journal of Dentistry.* 2023;134:104530.
49. Rutkūnas V, Gedrimienė A, Mischitz I, Mijiritsky E, Huber S. EPA Consensus Project Paper: Accuracy of Photogrammetry Devices, Intraoral Scanners, and Conventional Techniques for the Full-Arch Implant Impressions: A Systematic Review. *The European journal of prosthodontics and restorative dentistry.* 2023.
50. Mennito AS, Evans ZP, Nash J, Bocklet C, Lauer Kelly A, Bacro T, et al. Evaluation of the trueness and precision of complete arch digital impressions on a human maxilla using seven different intraoral digital impression systems and a laboratory scanner. *Journal of esthetic and restorative dentistry : official publication of the American Academy of Esthetic Dentistry [et al].* 2019;31(4):369-77.
51. Winkler J, Gkantidis N. Intraoral scanners for capturing the palate and its relation to the dentition. *Scientific Reports.* 2021;11(1):15489.
52. Bjelopavlovic M, Degering D, Lehmann KM, Thiem DGE, Hardt J, Petrowski K. Forensic Identification: Dental Scan Data Sets of the Palatal Fold Pairs as an Individual Feature in a Longitudinal Cohort Study. *Int J Environ Res Public Health.* 2023;20(3).
53. Oliva B, Sferra S, Greco AL, Valente F, Grippaudo C. Three-dimensional analysis of dental arch forms in Italian population. *Prog Orthod.* 2018;19(1):34.
54. Interpol. Disaster Victim Identification Guide 2018 [updated 2021.04.11. Available from: <https://www.interpol.int/How-we-work/Forensics/Disaster-Victim-Identification-DVI>.
55. Vanderveken A, Guha-Sapir D, McClean D, Cred, Unisdr. Poverty & Death: Disaster Mortality, 1996-2015. 2016.

56. Affairs UNOfD. Human Cost of Disasters. 2020.
57. Hableány hajóbaleset: Wikipédia; 2019 [updated 2021.02.09. Available from: https://hu.wikipedia.org/wiki/2019-es_budapesti_haj%C3%B3katasztr%C3%B3fa.
58. Ethiopian Airlines Flight 302: Wikipedia; 2019 [updated 2021.04.06. Available from: https://en.wikipedia.org/wiki/Ethiopian_Airlines_Flight_302.
59. 2016-os brüsszeli terrortámadás: Wikipédia; 2016 [updated 2019.04.11. Available from: https://hu.wikipedia.org/wiki/2016-os_br%C3%BCsszeli_terrort%C3%A1mad%C3%A1s.
60. 2016 Nice truck attack: Wikipédia; 2016 [updated 2021.03.31. Available from: https://en.wikipedia.org/wiki/2016_Nice_truck_attack.
61. 2016 Berlin truck attack: Wikipédia; 2016 [updated 2021.04.07. Available from: https://en.wikipedia.org/wiki/2016_Berlin_truck_attack.
62. 2017-es stockholmi terrortámadás: Wikipédia; 2017 [updated 2019.04.25. Available from: https://hu.wikipedia.org/wiki/2017-es_stockholmi_terrort%C3%A1mad%C3%A1s.
63. 2017-es katalóniai terrortámadások: Wikipédia; 2017 [updated 2019.04.11. Available from: https://hu.wikipedia.org/wiki/2017-es_katal%C3%B3niai_terrort%C3%A1mad%C3%A1sok.
64. Christchurch mosque shootings: Wikipédia; 2019 [updated 2021.04.10. Available from: https://en.wikipedia.org/wiki/Christchurch_mosque_shootings.
65. 2020-as bécsi terrortámadás: Wikipédia; 2020 [updated 2020.11.04. Available from: https://hu.wikipedia.org/wiki/2020-as_b%C3%A9csi_terrort%C3%A1mad%C3%A1s.
66. 2020 Beirut explosion: Wikipedia; 2020 [updated 2021.04.10. Available from: https://en.wikipedia.org/wiki/2020_Beirut_explosion.
67. Passenger train carrying 490 derails in Taiwan, killing at least 50 and injuring dozens: CNN; 2021 [updated 2021.04.03. Available from: <https://edition.cnn.com/2021/04/01/asia/taiwan-train-derail-intl-hnk/index.html>.
68. Angyal M, Petrétei D. Az Interpol DVI-protokoll-adaptációjával a hazai áldozatazonosítás fejlesztésének útján. NEMZETBIZTONSÁGI SZEMLE. 2019;7. évfolyam(1. szám):3-17.

69. Schuller-Götzburg P, Suchanek J. Forensic odontologists successfully identify tsunami victims in Phuket, Thailand. *Forensic science international*. 2007;171(2-3):204-7.
70. Schuller-Götzburg P, Suchanek J, Gugler J. Identifizierung der Tsunamiopfer im Thai Tsunami Victim Identification-Information Management Center (TTVI-IMC) in Phuket, Thailand. *Österreichische Zeitschrift für Stomatologie*. 2005;102:109-13.
71. 2023 Turkey–Syria earthquake: Wikipedia; 2023 [updated 2023.02.25. Available from: https://en.wikipedia.org/wiki/2023_Turkey%E2%80%93Syria_earthquake.
72. Derom C, Bakker E, Vlietinck R, Derom R, Berghe H, Thiery M, et al. Zygosity determination in newborn twins using DNA Variants 1985. 279-82 p.
73. Fraga MF, Ballestar E, Paz MF, Ropero S, Setien F, Ballestar ML, et al. From The Cover: Epigenetic differences arise during the lifetime of monozygotic twins. *Proceedings of the National Academy of Sciences*. 2005;102(30):10604-9.
74. Willis AJ, Myers L. A cost-effective fingerprint recognition system for use with low-quality prints and damaged fingertips. *Pattern Recognition*. 2001;34(2):255-70.
75. Petju M, Suteerayongprasert A, Thongpud R, Hassiri K. Importance of dental records for victim identification following the Indian Ocean tsunami disaster in Thailand. *Public Health*. 2007;121(4):251-7.
76. Sims CA, Berketa J, Higgins D. Is human identification by dental comparison a scientifically valid process? *Sci Justice*. 2020;60(5):403-5.
77. Adams BJ, Aschheim KW. Computerized Dental Comparison: A Critical Review of Dental Coding and Ranking Algorithms Used in Victim Identification. *J Forensic Sci*. 2016;61(1):76-86.
78. Hartung B, Rauschnig D, Schwender H, Ritz-Timme S. A simple approach to use hand vein patterns as a tool for identification. *Forensic science international*. 2020;307:110115.
79. El-Sayed MA, Abdel-Latif MA. Iris recognition approach for identity verification with DWT and multiclass SVM. *PeerJ Comput Sci*. 2022;8:e919.
80. Simon B, Farid AA, Freedman G, Vag J. Digital scans and human identification: Oral Health Group; 2021 [Available from: <https://www.oralhealthgroup.com/features/digital-scans-and-human-identification/>.

81. Allwood JS, Fierer N, Dunn RR. The Future of Environmental DNA in Forensic Science. *Appl Environ Microbiol.* 2020;86(2).
82. Monden C, Pison G, Smits J. Twin Peaks: more twinning in humans than ever before. *Human Reproduction.* 2021.
83. Martini M, Bufalari I, Stazi MA, Aglioti SM. Is That Me or My Twin? Lack of Self-Face Recognition Advantage in Identical Twins. *PLOS ONE.* 2015;10(4):e0120900.
84. Weber-Lehmann J, Schilling E, Gradl G, Richter DC, Wiehler J, Rolf B. Finding the needle in the haystack: Differentiating “identical” twins in paternity testing and forensics by ultra-deep next generation sequencing. *Forensic Science International: Genetics.* 2014;9:42-6.
85. Tao X, Chen X, Yang X, Tian J. Fingerprint recognition with identical twin fingerprints. *PLoS One.* 2012;7(4):e35704.
86. Tarnoki AD, Tarnoki DL, Forgo B, Szabo H, Melicher D, Metneki J, et al. The Hungarian Twin Registry Update: Turning From a Voluntary to a Population-Based Registry. *Twin research and human genetics : the official journal of the International Society for Twin Studies.* 2019;22(6):561-6.
87. Christiansen L, Frederiksen H, Schousboe K, Skytthe A, von Wurmb-Schwark N, Christensen K, et al. Age- and sex-differences in the validity of questionnaire-based zygosity in twins. *Twin Res.* 2003;6(4):275-8.
88. Heath AC, Nyholt DR, Neuman R, Madden PAF, Bucholz KK, Todd RD, et al. Zygosity Diagnosis in the Absence of Genotypic Data: An Approach Using Latent Class Analysis. *Twin Research.* 2012;6(01):22-6.
89. Meester JAN, Verstraeten A, Schepers D, Alaerts M, Van Laer L, Loeys BL. Differences in manifestations of Marfan syndrome, Ehlers-Danlos syndrome, and Loeys-Dietz syndrome. *Ann Cardiothorac Surg.* 2017;6(6):582-94.
90. Chen Y, Medioni G. Object modelling by registration of multiple range images. *Image and Vision Computing.* 1992;10(3):145-55.
91. Sharma G, Mathew T. One-Sided and Two-Sided Tolerance Intervals in General Mixed and Random Effects Models Using Small-Sample Asymptotics. *Journal of the American Statistical Association.* 2012;107(497):258-67.

92. Ferrario VF, Sforza C, Colombo A, Dellavia C, Dimaggio FR. Three-dimensional hard tissue palatal size and shape in human adolescents and adults. *Clin Orthod Res.* 2001;4(3):141-7.
93. Koo TK, Li MY. A Guideline of Selecting and Reporting Intraclass Correlation Coefficients for Reliability Research. *J Chiropr Med.* 2016;15(2):155-63.
94. Ulijaszek SJ, Kerr DA. Anthropometric measurement error and the assessment of nutritional status. *Br J Nutr.* 1999;82(3):165-77.
95. Stella O. Discriminant Analysis: An Analysis of Its Predictship Function. *Journal of Education and Practice.* 2019;10(5):8.
96. Boedeker P, Kearns NT. Linear Discriminant Analysis for Prediction of Group Membership: A User-Friendly Primer. *Advances in Methods and Practices in Psychological Science.* 2019;2(3):250-63.
97. Gan N, Xiong Y, Jiao T. Accuracy of Intraoral Digital Impressions for Whole Upper Jaws, Including Full Dentitions and Palatal Soft Tissues. *PLoS ONE.* 2016;11(7):e0158800.
98. Bishara SE, Jakobsen JR, Treder J, Nowak A. Arch width changes from 6 weeks to 45 years of age. *American journal of orthodontics and dentofacial orthopedics : official publication of the American Association of Orthodontists, its constituent societies, and the American Board of Orthodontics.* 1997;111(4):401-9.
99. Bell JT, Spector TD. A twin approach to unraveling epigenetics. *Trends Genet.* 2011;27(3):116-25.
100. Saadeh M, Macari A, Haddad R, Ghafari J. Instability of palatal rugae following rapid maxillary expansion. *European journal of orthodontics.* 2017;39(5):474-81.
101. Pedlar J. Healing following full thickness excision of human palatal mucosa. *Br J Plast Surg.* 1985;38(3):347-51.
102. Nagy Z, Simon B, Mennito A, Evans Z, Renne W, Vag J. Comparing the trueness of seven intraoral scanners and a physical impression on dentate human maxilla by a novel method. *BMC Oral Health.* 2020;20(1):97.
103. Vag J, Nagy Z, Simon B, Mikolicz A, Kover E, Mennito A, et al. A novel method for complex three-dimensional evaluation of intraoral scanner accuracy. *Int J Comput Dent.* 2019;22(3):239-49.

104. Nagare SP, Chaudhari RS, Birangane RS, Parkarwar PC. Sex determination in forensic identification, a review. *Journal of forensic dental sciences*. 2018;10(2):61-6.
105. Santos F, Guyomarc'h P, Bruzek J. Statistical sex determination from craniometrics: Comparison of linear discriminant analysis, logistic regression, and support vector machines. *Forensic science international*. 2014;245:204.e1-.e8.
106. Byers SN, Churchill SE, Curran B. Identification of Euro-Americans, Afro-Americans, and Amerindians from palatal dimensions. *J Forensic Sci*. 1997;42(1):3-9.
107. Burris BG, Harris EF. Identification of race and sex from palate dimensions. *J Forensic Sci*. 1998;43(5):959-63.
108. Simon B, Liptak L, Liptak K, Tarnoki AD, Tarnoki DL, Melicher D, et al. Application of intraoral scanner to identify monozygotic twins. *BMC Oral Health*. 2020;20(1):268.
109. Latham J, Ludlow M, Mennito A, Kelly A, Evans Z, Renne W. Effect of scan pattern on complete-arch scans with 4 digital scanners. *The Journal of prosthetic dentistry*. 2020;123(1):85-95.
110. Revell G, Simon B, Mennito A, Evans ZP, Renne W, Ludlow M, et al. Evaluation of complete-arch implant scanning with 5 different intraoral scanners in terms of trueness and operator experience. *The Journal of prosthetic dentistry*. 2021.
111. Deferm JT, Schreurs R, Baan F, Bruggink R, Merckx MAW, Xi T, et al. Validation of 3D documentation of palatal soft tissue shape, color, and irregularity with intraoral scanning. *Clin Oral Investig*. 2018;22(3):1303-9.
112. Vag J, Renne W, Revell G, Ludlow M, Mennito A, Teich ST, et al. The effect of software updates on the trueness and precision of intraoral scanners. *Quintessence Int*. 2021;0(0):0.
113. Camcı H, Salmanpour F. A new technique for testing accuracy and sensitivity of digital bite registration: A prospective comparative study. *Int Orthod*. 2021;19(3):425-32.
114. Balla SB. Forensic Dental Identification: Practice in Indian context compared to western countries. *Journal of Forensic science and medicine*. 2016:44-7.
115. Gupta L, editor *Role and importance of forensic odontology in identification* 2014.

9. Bibliography of the candidate's publications

Publications directly connected to the dissertation

In 2022

Simon, B., K. Aschheim, and J. Vág, *The discriminative potential of palatal geometric analysis for sex discrimination and human identification*. Journal of Forensic Sciences, 2022. 64(4). <https://doi.org/10.1111/1556-4029.15110>

In 2020

Simon B, Lipták L, Lipták K, Tárnoki ÁD, Tárnoki DL, Melicher D, Vág J: *Application of intraoral scanner to identify monozygotic twins*. BMC Oral Health 2020, 20(1):268. <https://doi.org/10.1186/s12903-020-01261-w>

Total impact factor: 4,357

Total citation:

9 (data from MTMT 2023, June)

18 (data from Google Scholar 2023. June)

Publications indirectly connected to the dissertation

In 2023

Simon B, Mangano FG, Pál A, Simon I, Pellei D, Shahbazi A, et al. *Palatal asymmetry assessed by intraoral scans: effects of sex, orthodontic treatment, and twinning. A retrospective cohort study*. BMC Oral Health. 2023;23(1):305. <https://doi.org/10.1186/s12903-023-02993-1>

Mikolicz A, **Simon B**, Gáspár O, Shahbazi A, Vag J. *Reproducibility of the digital palate in forensic investigations: a two-year retrospective cohort study on twins*. Journal of Dentistry. 2023;135:104562. <https://doi.org/10.1016/j.jdent.2023.104562>

In 2022

Borbola D, Berkei G, **Simon B**, Romanszky L, Sersli G, DeFee M, et al. *In vitro comparison of five desktop scanners and an industrial scanner in the evaluation of an intraoral scanner accuracy.* Journal of Dentistry. 2022:104391. <https://doi.org/10.1016/j.jdent.2022.104391>

In 2021

Simon B, Farid AA, Vág J: *A preventív és proaktív fogászati azonosítás bevezetése és jelentősége tömegkatasztrófa áldozat azonosításkor.* Scientia et Securitas 2021, 2(1):123-134. <https://doi.org/10.1556/112.2021.00004>

Simon, B., A. A. Farid, G. Freedman and J. Vag (2021). *Digital scans and human identification.* Oral Health Journal July 1. Oral Health Journal 111:7 36-39 <https://www.oralhealthgroup.com/features/digital-scans-and-human-identification/>

Revell G, **Simon B**, Mennito A, Evans ZP, Renne W, Ludlow M, Vág J: *Evaluation of complete-arch implant scanning with 5 different intraoral scanners in terms of trueness and operator experience.* The Journal of prosthetic dentistry 2021. <https://doi.org/10.1016/j.prosdent.2021.01.013>

In 2020

Simon B: *Az igazságügyi fogorvosszakértés múltja, jelene és jövője.* Kaleidoscope history 2020, 10(21):156-164. <https://doi.org/10.17107/kh.2020.21.156-164>

Simon B: *Semmelweis 250 Klinikai Konferencia összefoglaló.* Scientia et Securitas ScientSec 2020, 1(1):71. <https://doi.org/10.1556/112.2020.00012>

Vág, J., Nagy, Z., Bocklet, C. et al. *Marginal and internal fit of full ceramic crowns milled using CAD/CAM systems on cadaver full arch scans.* BMC Oral Health 20, 189 (2020). <https://doi.org/10.1186/s12903-020-01181-9>

Nagy, Z., **Simon, B.**, Mennito, A. et al. *Comparing the trueness of seven intraoral scanners and a physical impression on dentate human maxilla by a novel method.* BMC Oral Health 20, 97 (2020). <https://doi.org/10.1186/s12903-020-01090-x>

In 2019

Simon B, Vág J: *Mire képes a chairside CAD/CAM kvadráns rehabilitációnál?* Dental Hírek 2019, XIII.(1.):54-59.

Vág, J., Nagy, Z., **Simon, B.**, Mikolicz, Á., Kövér, E., Mennito, A., Evans, Z., & Renne, W. (2019). *A novel method for complex three-dimensional evaluation of intraoral scanner accuracy.* International Journal of computerized dentistry, 22(3),239–249.

In 2018

Nagy, Z. A., **Simon, B.**, Tóth, Z., & Vág, J. (2018). *Evaluating the efficiency of the Dental Teacher system as a digital preclinical teaching tool.* European journal of dental education: official journal of the Association for Dental Education in Europe, 22(3), e619–e623. <https://doi.org/10.1111/eje.12365>

Total impact factor: 25,059

Total citation:

106 (data from MTMT 2023, June)

155 (data from Google Scholar 2023. June)

10. Acknowledgements

I would like to express my heartfelt gratitude to Professor János Vág, my mentor and supervisor, for his invaluable help, guidance, and trust throughout this journey. His expertise and support, along with his assistance in statistical calculations, have been instrumental in the success of this research.

I am deeply thankful to my wife, Szonja, whose unwavering support and encouragement have been a constant source of strength, especially during the most challenging moments of this endeavor.

I extend my appreciation to Dr. Klaudia Lipták and Dr. Laura Lipták, who have transitioned from being my students to becoming my colleagues. They played a significant role in sparking the initial idea for this research.

I am indebted to the Hungarian Twin Registry, particularly Dr. Ádám Tárnoki, Dr. Dávid Tárnoki, and Dr. Dóra Melicher, for their assistance in recruiting twins and facilitating the progress of this study.

My heartfelt thanks go out to the twins who participated in this research, as well as to Dr. Ajang Armin Farid, the DVI team leader of the Hungarian Forensic Odontology Unit. Thanks to his support, I had the opportunity to connect with international experts and share the outcomes of our research with the world. I am also grateful to our French and American DVI colleagues for their collaboration and support.

I wish to acknowledge the support of the Internal Affairs Science Council, the Innovation Directorate of Semmelweis University, the National Research, Development and Innovation Office, and the Erasmus Office. Their financial support and travel funding have made a significant contribution to the colorful and diverse nature of my PhD dissertation.

I would like to express my appreciation to Professor Gábor Varga and Dean Miklós Kellermayer for their guidance and encouragement. My gratitude also extends to the students, assistants and colleagues who were involved in this research, as well as to my parents and family for their unwavering support.